A survey on dielectric elastomer actuators for soft robots

2017 Bioinspir. Biomim. 12 011003

(http://iopscience.iop.org/1748-3190/12/1/011003)

IOP Publishing Bioinspir. Biomim. 12 (2017) 011003 doi:10.1088/1748-3190/12/1/011003

Bioinspiration & Biomimetics

RECEIVED
22 May 2016

REVISED
31 October 2016

ACCEPTED FOR PUBLICATION
1 November 2016

PUBLISHED
23 January 2017

TOPICAL REVIEW

A survey on dielectric elastomer actuators for soft robots

Guo-Ying Gu[1,3], **Jian Zhu**[2], **Li-Min Zhu**[1] **and Xiangyang Zhu**[1]

[1] State Key Laboratory of Mechanical System and Vibration, School of Mechanical Engineering, Shanghai Jiao Tong University, 200240, People's Republic of China
[2] Department of Mechanical Engineering, National University of Singapore, 9 Engineering Drive 1, 117576, Singapore
[3] Author to whom any correspondence should be addressed

E-mail: guguoying@sjtu.edu.cn

Keywords: soft robots, dielectric elastomer actuators, electromechanical modeling, design, control

Abstract

Conventional industrial robots with the rigid actuation technology have made great progress for humans in the fields of automation assembly and manufacturing. With an increasing number of robots needing to interact with humans and unstructured environments, there is a need for soft robots capable of sustaining large deformation while inducing little pressure or damage when maneuvering through confined spaces. The emergence of soft robotics offers the prospect of applying soft actuators as artificial muscles in robots, replacing traditional rigid actuators. Dielectric elastomer actuators (DEAs) are recognized as one of the most promising soft actuation technologies due to the facts that: i) dielectric elastomers are kind of soft, motion-generating materials that resemble natural muscle of humans in terms of force, strain (displacement per unit length or area) and actuation pressure/density; ii) dielectric elastomers can produce large voltage-induced deformation. In this survey, we first introduce the so-called DEAs emphasizing the key points of working principle, key components and electromechanical modeling approaches. Then, different DEA-driven soft robots, including wearable/humanoid robots, walking/serpentine robots, flying robots and swimming robots, are reviewed. Lastly, we summarize the challenges and opportunities for the further studies in terms of mechanism design, dynamics modeling and autonomous control.

1. Introduction

Since the development of the Unimate robot in 1959 by G Devol and J Engelberger, industrial robots have taken on a variety of automatic assembling and manufacturing tasks that are generally difficult, dangerous, or impractical for humans [1–3]. The industrial robots are generally made of metal and plastic materials that are inherently 'rigid'. It is such 'rigid' feature that makes the robots perfect for repetitive works with fine accuracies in well-defined environments. However, when there are unknown external constrains or obstacles, this kind of robots is generally difficult to change their shapes to adapt to the unstructured environment. In the field of conventional industrial robots, motion planner and compliant control [4–7] have been investigated to realize the compliance of the robots. Nevertheless, the natural world is different. If we look at humans and other animals, their 'bodies' are usually built from the soft materials, such as the muscles, skins and fiber-like tissues, which are safe and compatible to interact with humans or negotiating confined environments.

With the field of robotics expanding beyond manufacturing automation into health care, field exploration, or human-robot cooperative manipulation, soft robots that are capable of large deformation and maneuvering through unstructured constrained spaces without inducing damaging internal pressures and stress concentrations, are emerging as a new frontier of multidisciplinary in terms of engineering, materials, mechanics, physics, chemistry, biology and robotics.

During the past decade, soft robotics becomes a growing new field and researchers have developed different kinds of soft robots with different actuation technologies and mechanisms [8–12]. The development of soft robots is generally bioinspired or biomimetic with the capabilities of large and continuum deformation with theoretically an infinite number of degree-of-freedoms. Considering the differences of

actuation technologies, soft robots can be mainly divided into two categories.

The first category is based on the tendon-driven actuation, which is also termed as continuum robots in order to distinguish the discrete and serpentine robots with rigid links [13]. Depending on the selections of the tendon-driven mechanism with either intrinsic actuators, extrinsic actuators or intrinsic–extrinsic hybrid actuators, the continuum robots can be designed to be elastic with infinite degrees of freedom (DOFs), which have been successfully used in medicine, search and rescue fields. However, such continuum robots usually utilize the traditional motors and transmission mechanism (such as gears and ball screws), leading to not real soft bodies. The reader may refer to [14, 15] for a recent review of this kind of robots.

The second category is based on the soft smart materials actuation. Different from the tendon-driven actuation with the traditional motors and transmission mechanism, the smart materials can directly convert physical stimuli, such as force, electrical, thermal, magnetic, light or chemical signal into a physical displacement. The commonly used soft smart materials for soft robots include the shape memory alloys (SMAs), shape memory polymers (SMPs), pneumatic fiber braids or elastomeric polymers, hydrogels [16] and electroactive polymers (EAPs).

SMAs and SMPs are a kind of materials capable of undergoing large strain when heated [17–19]. Laschi's group from Scuola Superiore SantAnna in Italy has made great efforts in developing soft octopus arms with SMAs [20, 21]. However, the temperature-dependent nature makes precisely control of SMAs difficult. Pneumatic fiber braids or elastomeric polymers for soft robots have been studied for decades [22] and have recently re-attracted significant attention due to the promising achievements of Whitesides' group from Harvard University in USA [23–25]. However, external air compressors are necessary and the response speed is usually limited by the capability to pump air into and out of the actuators. EAPs are a kind of soft materials capable of changing sizes and/or shapes in response to the electrical stimuli, and are an emerging type of soft actuation technology in the field of soft robotics due to their ability of mimicking the properties of natural muscle. The reader may refer to the books [26, 27] for the complete understanding of different EAP based transducers. Considering the differences of stimuli methods, soft EAPs are typically classified into two classes: ionic EAPs and electronic EAPs. It is worthy of mentioning that the ionic EAPs are usually limited due to their poor coupling efficiencies and relatively slow actuation speeds [28, 29], which may hinder their applications in soft robots. On the other hand, dielectric elastomers, a kind of electronic EAPs, are more promising in the emerging scientific field of soft robotics due to the advantages of light weight, high deformation, high energy density, fast response and inherent soft nature [11, 29, 30]. It should be noted that semi-active actuation like magneto- or electro-rheological foam/elastomers and granular jamming technologies have been employed for developing soft robots as an alternative option, which are not classified in this paper, and may refer to [19] for an overview.

In this paper, we intend to survey and discuss the recent progresses on soft robots using dielectric elastomer actuators (DEAs). Our survey is motivated by several factors. First, several years have elapsed since the publishment of some important and most often-cited books on electroactive transducers, for instance, edited by Bar-Cohen [26] and Carpi *et al* [27], during which many important advancements have been made. Second, few attentions are paid on dynamic modeling, control and the application of DEAs to soft robots in these two books [26, 27]. Third, the progress and achievement mainly focus on the issues of materials, mechanics and physics. With the rapid development of the soft robots, this topic may draw more attentions in the society of robotics and automation. In this sense, an overview and recent progress of the representative and featured works in the field of DEAs, emphasizing the key points of work principle, modeling, control and robotic applications, are presented. We also aim to highlight challenges and new opportunities for the further studies from our analysis and perspective in terms of mechanism design, dynamics modeling and autonomous control. The remainder of this survey is organized as follows: section 2 introduces the descriptions, working principle and key components of the dielectric elastomer actuators. In section 3, electromechanical modeling approaches for dielectric elastomer actuators are presented and section 4 reviews the soft robots using dielectric elastomer actuators. Finally, challenges and opportunities are summarized in section 5.

2. Dielectric elastomer actuators

DEAs are promising for applications in the field of soft robotics due to the unique combination of the advantages of large deformation (>100%), high energy density (>3.4 MJ m^{-3}), fast responses (on the order of millisecond), lightweight (close to water) and low cost (hundreds of commercial elastomer products). Specially, another key benefit is that dielectric elastomers are a kind of motion-generating materials that resemble natural muscle of humans in terms of force, strain (displacement per unit length or area) and actuation pressure/density compared to other competitors as illustrated in figure 1.

2.1. Working principle

Dielectric elastomers are a kind of soft electroactive materials, which means the external electrical stimulus causes the elastomers to deform in dimensions and/or

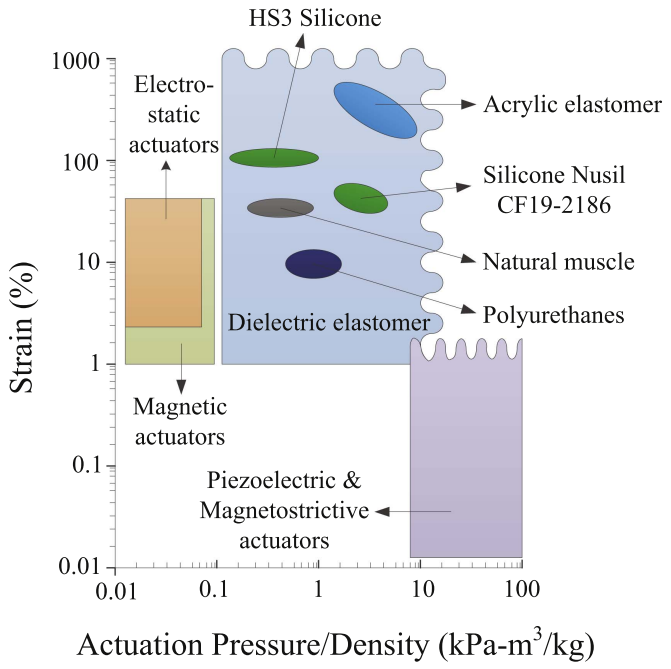

Figure 1. Illustration of actuation strain versus actuation pressure/density for various actuation technologies.

shape, and such deformation leads to a mechanical function. As a result, dielectric elastomers can be applied to design actuators. On the other hand, when a deformation or mechanical loading is applied on a dielectric elastomer, a change in capacitance can be detected as well because of its capacitive nature. Thus, it is also possible to make the dielectric elastomer a sensor. In this survey, we mainly focus on the dielectric elastomers as actuators.

Electrical induced deformation of solid materials was originated in the late-18th century after the invention of Leyden jars by the Italian experimenter Felice Fontana [31, 32]. Intense investigations on such electrical deformation in the volume of the Leyden jar were then performed in the late 19th century. In 1880, Röntgen presented an experiment [32, 33]: a 16 cm wide and 100 cm long stripe of natural rubber was pre-stretched by a weight to twice its initial length; upon electrification with sprayed-on electric charges onto the rubber, length changes on the order of several centimeters were able to be observed in the experiment. This experiment is a simple but milestone to illustrate the electrical deformation of a natural rubber. After a long time until the early-21th century, the concept of electrically actuated large-deformation dielectric elastomers is again at the forefront of emerging soft robots with the development of technology.

Although dielectric elastomers allow for the operation of actuators without attached electrodes, where charges are directly sprayed on the elastomer surface as reported by Röntgen, voltage controlled DEAs are more promising and universal in applications so far. Without losing generality, the following descriptions on DEAs are based on the voltage controlled mode if there is no specific remark.

In general, DEAs consist of a thin membrane of dielectric elastomer, which is sandwiched between two compliant electrodes. Therefore, DEAs are essentially compliant variable capacitors. The compliant electrodes are made of even softer substance with the mechanical stiffness lower than that of the dielectric elastomers [34]. DEAs operate on the principle of the so-called electrostatic deformation. When an electric field is applied across the electrodes, the charges pass through an external conducting wire from one electrode to the other. The resulting electrostatic force between the opposite charges on the two electrodes compresses the membrane in thickness. Since the dielectric elastomers are essentially incompressible, such compression results in a concomitant stretch in the planar area of the membrane. Both shape changes convert electrical energy to mechanical energy and provide the actuation mechanism [35]. Figure 2 illustrates such working principle of actuation.

A landmark discovery was by Pelrine and colleagues [35, 36] reported 16 years ago that the applied voltage can cause the dielectric elastomers to achieve high-speed and giant strain over 100%. Due to the capability of large strain, DEAs are widely recognized as the most promising potential for creating artificial muscles. During the past decade, the study of DEAs is rapidly broadening to diverse applications [11, 15, 31, 37] with the urgent necessary of soft actuators. These applications have also introduced renewed interests in the design and theory of coupled large deformation and electric field considering both the static and dynamic behaviors.

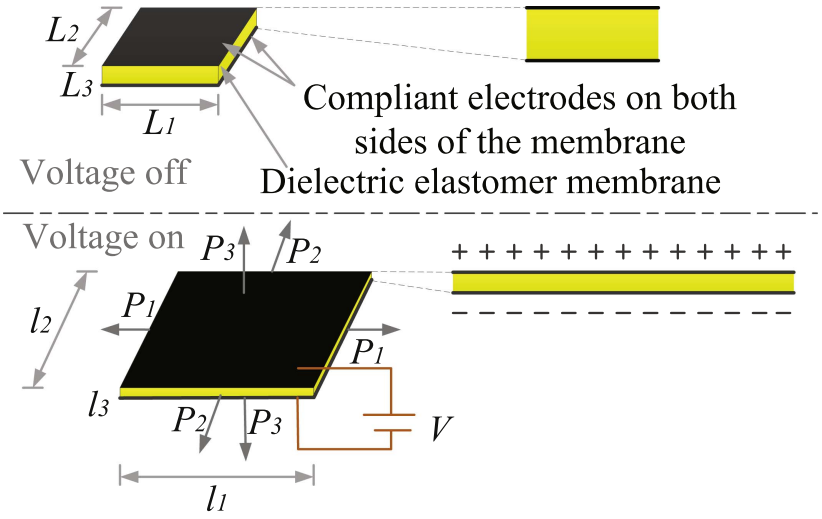

Figure 2. Illustration of working principle of DEA. When a voltage is applied across a dielectric elastomer membrane coated on both sides with compliant electrodes, electrostatic forces are produced to compress the membrane in the thickness and expand it in the area.

2.2. Dielectric elastomer materials

It can be seen from figure 2 that the most important component of DEAs is the thin membrane made of dielectric elastomers. In the dielectric elastomer research, materials are needed with a wide range of elastic moduli, combined with very low viscosity and electrical conductivity, high dielectric constant and breakdown strength [37]. During the last two decades, a large number of elastomeric materials have been tested. The commonly used elastomers can be roughly classified into three groups, i.e., polyurethanes (PUs), acrylics and silicones.

Due to the fact that PUs generally have larger force outputs and higher dielectric constant, DEAs made of PU films can be actuated at lower electric fields. However, this kind of DEAs has the limitation of small strain.

Since the report of Pelrine and colleagues [35, 36], acrylics seem to be the most promising selection for the large-strain DEAs. One popular reason of acrylics also lies in the fact that there is low-cost commercially available 3M VHB acrylic elastomer (such as the most used VHB 4910 and VHB 4905). Recently, DEAs with the prestretched 3M VHB acrylic elastomer have been widely reported to achieve giant voltage-induced linear strains over 380% [38], area strains more than 1000% [39, 40]. However, the acrylics exhibit strong viscoelastic nonlinearities [41, 42], which usually influence the performance of DEAs if the viscoelasticity cannot be well accounted for.

DEAs with silicone elastomers show modest actuation strain, which is larger than DEAs with PUs, but smaller than DEAs with acrylics. However, silicone elastomers have the advantage of lower viscoelasticity than acrylics and are reported to be operated at higher frequencies with lower losses [29]. On the other hand, similar to acrylics, silicones have a relatively low dielectric constant as well, which, therefore, requires higher electric fields for large strains.

2.3. Compliant electrodes

As shown in figure 2, another important component of DEAs is the compliant electrode. The term 'compliant' means the ability of a thin, conducting electrode to synchronously follow the large strains of the elastomer membrane, but without generating an opposing stress or losing conductivity [43].

Therefore, the electrode generally has the following properties: conductive, highly compliant, thin in thickness compared to the elastomer membrane, good adhesion to the membrane, low resistance and high surface density even under large strain, easy to be painted with high resolution and durable, but do not significantly impacting the mechanics of the actuators. In the literature, the commonly used electrode materials include carbon grease, graphite and carbon powder, and metallic thin film [29, 30, 43–46].

In these solutions, carbon grease electrodes are the most popular selection since they are cheap and easy to apply on most dielectric elastomers with excellent adhesion capability. They were also reported to provide good conductivity even at very high strains without the migration. However, the main drawback of the grease electrodes is messy to handle in fabrication.

On the contrast, dry graphite and carbon powder are easy to handle, which are also cheap and easy to apply. They are more suitable for multilayered DEAs than carbon grease electrodes. However, the conducting performance becomes worse with higher strain due to the loss of electrical contact.

Metallic thin-film electrodes are considered for utilization due to the advantages of: (i) stable electrical resistance, (ii) being able to expand in the corrugated format. However, corrugated metal thin-film

electrodes are generally stiffened in the transverse axial direction and are consequently almost inextensible in that direction. On the other hand, the metallic electrodes can only be used with relatively small strains.

The above compliant electrodes are electronic conductors and nontransparent. As an alternative, a new compliant electrode was recently invented by Keplinger and colleagues [47] using ionic conductors that are highly stretchable, fully transparent to light of all colors, and capable of operation at frequencies beyond 10 kHz and voltages above 10 kV. By placing two electrodes (electronic conductors), an electrolyte (ionic conductor), and a dielectric elastomer in series, a novel DEA was designed, which is demonstrated to generate large strains and a transparent loudspeaker that produces sound over the entire audible range.

3. Electromechanical modeling approaches

As addressed in the previous section, the actuation mechanism of DEAs is the produced electrostatic stress on the thin membrane between the two charged electrodes due to the applied voltage, which thus generates the mechanical response. In this section, the methods to predict this electromechanical response of DEAs are discussed and compared.

3.1. Early electromechanical modeling approach

The first physical model to describe the electromechanical behaviors of DEAs is developed by Pelrine and colleagues [35, 36]. When subjected to a voltage V across a prestreched DEA, the resulting electrostatic stress is described as a function of the total permittivity of the material and the square of the applied electric field E with the following form

$$p = \varepsilon_0 \varepsilon_r E^2 = \varepsilon_0 \varepsilon_r \left(\frac{V}{h}\right)^2, \quad (1)$$

where p represents the effective compressive stress, known as Maxwell stress, ε_0 and ε_r are absolute permittivity and the relative permittivity of dielectric elastomers, respectively, and h is the thickness of the actuated membrance between the opposite electrodes. Since the planar stretching in DEAs is coupled to the thickness compression, the effective compressive stress in (1) is twice the stress normally calculated for two rigid, charged capacitor plates.

In (1), the dielectric elastomer is assumed to be ideal for uniform electrical charges on infinitely large electrodes and uniform film thickness. In addition, the dielectric behavior of the elastomer is liquid-like and unaffected by deformation. This model has been well experimentally verified and used widely in the literature to describe electromechanical behavior of the DEAs [27, 29, 32, 48–56].

According to (1), Pelrine and colleagues further provided a simple method to predict the DEA strains. For low strains (e.g., <20%), the thickness strain s_z is approximated as [35, 36].

$$s_z = -p/Y = -\varepsilon_0 \varepsilon_r \left(\frac{V}{h}\right)^2 / Y, \quad (2)$$

where Y is the elastic modulus relating to the strain. For high strain, the electromechanical energy density is used to estimate the the thickness strain s_z as follows

$$s_z = e^{-w_e/p} - 1, \quad (3)$$

where w_e is the electromechanical energy density, defined as the amount of electrical energy converted to mechanical energy per unit volume of the DEA for one cycle. Due to the homogeneity of the stretch and the incompressibility of the ideal elastomers, the strains on the plane can be further obtained based on thickness strain in (2) or (3).

It can be seen from (1) that the stress is proportional to the relative dielectric constant of the dielectric elastomers and inversely proportional to the thickness of the elastomer membrane. Therefore, the electric field across the thickness increases as the thickness of the membrane reduces after the voltage is applied to the DEA. This positive feedback may cause the elastomer to thin down drastically, resulting in an electrical breakdown or electromechanical instability and limiting strain performance of DEA. In addition, viscoelasticity is another inherent nonlinear behavior in dielectric elastomers that significantly influences the actuation of DEAs. It should be noted that Pelrine's approach described in (1)–(3) is pioneered and well-known in the field of DEAs for understanding and predicting the electromechanical response. However, it can not be effectively applied to account for the large-deformed nonlinearity and nonlinear elasticity of DEAs.

3.2. Energy-based electromechanical modeling approach

Inspired by the energy-based analytical approaches to account for the large-deformation nonlinearity and nonlinear elastic behaviors of rubber-like materials [57–63], researchers have made many efforts in the field of DEAs.

The early representative works by combining the theories of Maxwell stress and hyperelastic material models include Kofod [43], Kim *et al* [64], Goulbourne *et al* [65], Wissler and Mazza [66], Plante and Dubowsky [67]. In [43], three kinds of hyperelastic material models, i.e., the Hooke, neo-Hookean and Ogden models, were adopted to describe the one-dimensional voltage-strain relation of a DEA. In [64], the pre-straining influences on the performance of DEAs were investigated with a Mooney–Rivlin model. In [65], the Ogden strain energy function was employed to reliable electro-elastic modeling of a dielectric elastomer diaphragm for a prosthetic blood pump. In [66], an analytical method was developed to study the deformation of a circular DEA using three hyperelastic strain energy models (i.e., Yeoh, Ogden and Mooney–Rivlin models) coupled with quasi-linear viscoelasticity. In [67], an analytical model that

incorporated four fundamentals effects in terms of large deformations, nonlinear elastic behavior, viscoelasticity and variable dielectric strength was developed to predict the area stretch of DEAs as a function of film mechanical prestretch, applied voltage, speed of actuation, and working load. The more interesting result of Plante and Dubowsky's work [67] lies in the fact the developed model can predict DEA's failure modes including pull-in, dielectric strength, and material strength.

It can be seen that energy-based analytical approaches are effective to predict the large-deformation nonlinearity and nonlinear elastic behaviors in DEAs. However, there is no a general frame to combine them together. Based on the accumulated works, a general theory is recently proposed by Suo and colleagues [55, 68–70] from Harvard University, America, by coupling large deformation and electric potential to modeling the electromechanical behaviors of DEAs within the framework of continuum mechanics and thermodynamics. In the following, we give a detailed introduction of this theory for electromechanical modeling of DEAs.

3.3. A general electromechanical modeling frame

Considering a DEA as shown in figure 2, the geometric dimensions in the reference state are $L_1 \times L_2 \times L_3$. In the current state, the elastomer is subject to mechanical forces P_1, P_2, P_3, and an applied voltage V. The geometric dimensions become as $l_1 \times l_2 \times l_3$. For easy understanding of the following development, the stretch ratios on each direction are defined as $\lambda_1 = l_1/L_1$, $\lambda_2 = l_2/L_2$ and $\lambda_3 = l_3/L_3$. In addition, the electric charges on both electrodes are assumed to be Q and the Helmholtz free energy of the elastomer membrane is F.

3.3.1. Framework of equilibrium thermodynamics

Based on the energy balance, the increase of the free energy δF of the elastomer membrane equals to the work done by the mechanical forces $P_1\delta l_1 + P_2\delta l_2 + P_3\delta l_3$ and the work done by the battery $\Phi\delta Q$, satisfying,

$$\delta F = P_1\delta l_1 + P_2\delta l_2 + P_3\delta l_3 + \Phi\delta Q. \tag{4}$$

It should be noted that the condition of equilibrium in (4) holds for arbitrary small variations of the four independent variables l_1, l_2, l_3 and Q [34].

Define the nominal density of the Helmholtz free energy as

$$W = F/(L_1L_2L_3). \tag{5}$$

Hence, the increase of the density of the free energy can be obtained through dividing (4) by the volume $L_1L_2L_3$ of the elastomer on both sides,

$$\begin{aligned}\delta W = {} & (\sigma_1 + DE)\lambda_2\lambda_3\delta\lambda_1 + (\sigma_2 + DE)\lambda_1\lambda_3\delta\lambda_2 \\ & + \sigma_3\lambda_1\lambda_2\delta\lambda_3 + \lambda_1\lambda_2\lambda_3 E\delta D\end{aligned} \tag{6}$$

with

$$\sigma_1 = P_1/(l_2l_3), \tag{7}$$

$$\sigma_2 = P_2/(l_1l_3), \tag{8}$$

$$\sigma_3 = P_3/(l_1l_2), \tag{9}$$

$$E = V/l_3, \tag{10}$$

$$D = Q/(l_1l_2), \tag{11}$$

where σ_1, σ_2 and σ_3 represent the true stresses, E and D denote true electric field and electric displacement, respectively.

Without losing generality, the nominal density of the Helmholtz free energy W depends on the strains λ_1, λ_2, λ_3 and polarization displacement D. In this sense, W can be prescribed as a function of the four independent variables λ_1, λ_2, λ_3 and D as follows

$$W = W(\lambda_1, \lambda_2, \lambda_3, D). \tag{12}$$

Substituting (12) into (6), it is straightforward to obtain

$$\begin{aligned}&\left(\frac{\partial W}{\partial \lambda_1} - (\sigma_1 + DE)\lambda_2\lambda_3\right)\delta\lambda_1 \\ &\quad + \left(\frac{\partial W}{\partial \lambda_2} - (\sigma_2 + DE)\lambda_1\lambda_3\right) \\ &\delta\lambda_2 + \left(\frac{\partial W}{\partial \lambda_3} - \sigma_3\lambda_1\lambda_2\right)\delta\lambda_3 \\ &\quad + \left(\frac{\partial W}{\partial D} - \lambda_1\lambda_2\lambda_3 E\right)\delta D = 0.\end{aligned} \tag{13}$$

Considering the fact that the condition of equilibrium in (13) holds for arbitrary small variations of the four independent variables δl_1, δl_2, δl_3 and δQ, the following constitutive laws can be derived

$$\sigma_1 = \frac{\partial W(\lambda_1, \lambda_2, \lambda_3, D)}{\lambda_2\lambda_3\partial\lambda_1} - DE, \tag{14}$$

$$\sigma_2 = \frac{\partial W(\lambda_1, \lambda_2, \lambda_3, D)}{\lambda_1\lambda_3\partial\lambda_2} - DE, \tag{15}$$

$$\sigma_3 = \frac{\partial W(\lambda_1, \lambda_2, \lambda_3, D)}{\lambda_1\lambda_2\partial\lambda_3}, \tag{16}$$

$$E = \frac{\partial W(\lambda_1, \lambda_2, \lambda_3, D)}{\lambda_1\lambda_2\lambda_3\partial D}. \tag{17}$$

It should be noted that the condition $\delta Q = Dl_2\delta l_1 + Dl_1\delta l_2 + l_1l_2\delta D$ is utilized in the above derivation.

Since σ_1, σ_2, σ_3 and E depend on P_1, P_3, P_3 and V, (14)–(17) provide the constitutive equations relating the forces and voltage with the deformations in the terms of true quantities in the current state of a DEA.

3.3.2. Ideal dielectric elastomers

Considering the elastomer membrane in DEAs is the ideal dielectric elastomer, the following two assumptions should be obeyed [34]:

(A1) The dielectric elastomers is incompressible, i.e.,

$$\lambda_1\lambda_2\lambda_3 = 1. \tag{18}$$

(A2) The dielectric behavior of the elastomer membrane is exactly the same as that of poly melt, that is, the electric displacement relates to the electric field as,

$$D = \varepsilon E, \tag{19}$$

where the permittivity of the elastomer $\varepsilon = \varepsilon_0\varepsilon_r$ is a constant independent of deformation.

With these two assumptions, the nominal density of the Helmholtz free energy in (12) can be expressed as

$$W(\lambda_1, \lambda_2, D) = W_s(\lambda_1, \lambda_2) + D^2/(2\varepsilon), \tag{20}$$

where $W_s(\lambda_1, \lambda_2)$ represents the Helmholtz free energy associated with the stretch of the membrane; $D^2/2\varepsilon$ refers to the Helmholtz free energy associated with the polarization of the elastomer.

Then, the constitutive equations of DEAs in (14)–(17) can be re-expressed as

$$\sigma_1 - \sigma_3 = \frac{\lambda_1\partial W_s(\lambda_1, \lambda_2)}{\partial\lambda_1} - \varepsilon E^2, \tag{21}$$

$$\sigma_2 - \sigma_3 = \frac{\lambda_2\partial W(\lambda_1, \lambda_2)}{\partial\lambda_2} - \varepsilon E^2. \tag{22}$$

It should be mentioned that the first terms in the right hand side of (21) and (22) are the contribution to the mechanical stress due to the change of entropy associated with the stretch of the polymer network of the elastomers, while the second term is due to the applied voltage. In addition, once the function W_s is given, the constitutive models (21) and (22) are able to analyze the mechanical response of the DEAs. In the literature, exclusive simulation and experimental results that can verify the effectiveness of these equations have been reported, for instance, in [50, 55, 68, 69, 71–73].

Furthermore, the different electromechanical instabilities, such as the thinning and pull-in, snap-through, wrinkle, creasing and cavitation can be comprehensively accounted for with the Suo's approach. For a systematic understanding of different modes of instabilities, one may refer to a recent survey in [74].

3.4. Elastic material models

In the theory of rubber elasticity, there are a large number of well-tested functions for the elastic energy due to the deformation of the elastomer, for instance, neo-Hookean, Mooney–Rivlin, Yeoh, Gent, Ogden, and Arruda–Boyce models [57–63]. In this survey, we just introduce the three commonly used elastic models (i.e., neo-Hookean, Gent and Ogden models) in the field of DEAs.

3.4.1. Neo-Hookean model

The free energy density described by the neo-Hookean model of an incompressible hyperelastic material takes the form of

$$W_s = \frac{\mu}{2}(\lambda_1^2 + \lambda_2^2 + \lambda_3^2 - 3), \tag{23}$$

where μ is the small-strain shear modulus, which is a material constant (related to Youngs modulus). This free energy is due to the change of entropy when polymer chains are stretched [34, 60].

The neo-Hookean model is a hyperelastic material model that can be used for predicting the stress–strain behavior of materials. The benefit of the neo-Hookean model is its simple structure with only one material parameter μ, which is common in the early time for modeling of DEAs [43, 69, 75–77]. For most elastomers, the relation between the applied stress and strain is initially linear, but may change to nonlinear after a certain point at the stress–strain curve. This situation generally happens in the dielectric elastomers, which has a crosslinked network of long-chained polymers. However, each polymer chain may have a finite length, sometimes known as the extension limit [62]. When the polymer chains approach the stretch limit, the elastomer may stiffen sharply. In this case, the neo-Hooken model is not applicable.

3.4.2. Gent model

Contrast to the neo-Hookean model, the Gent model can predict the strain-stiffening effect, which was introduced by Gent in 1996 [63]. For the incompressible elastomers, the free energy density described by the Gent model can be expressed as

$$W_s = -\frac{\mu J_{lim}}{2}\log\left(1 - \frac{\lambda_1^2 + \lambda_2^2 + \lambda_3^2 - 3}{J_{lim}}\right), \tag{24}$$

where μ is the small-strain shear modulus, similar to the neo-Hookean model in (23) and J_{lim} is a constant related to the limiting stretch, which can describe the strain-stiffening effect. Recently, the Gent model has been one of the most popular models to predict the behaviors of DEAs [73, 78–84].

It can be seen that the Gent model also has the advantage of the simple structure with only two material parameter μ and J_{lim}. In addition, when $J_{lim} \to \infty$, the Gent model (24) reduces to the neo-Hookean model (23) according to the Taylor expansion. When $\lambda_1^2 + \lambda_2^2 + \lambda_3^2 - 3/J_{lim} \to 1$, the free energy W_s will diverge, and the elastomer approaches its limiting stretch.

3.4.3. Ogden model

Ogden model is another popular hyperelastic material model in the theory of rubber elasticity, which was proposed by Ogden in 1972 [59]. The free energy density of an incompressible hyperelastic material described by the Ogden model has the form of

$$W_s = \sum_{i=1}^{N}\frac{\mu_i}{\alpha_i}(\lambda_1^{\alpha_i} + \lambda_2^{\alpha_i} + \lambda_3^{\alpha_i} - 3), \tag{25}$$

where μ_i and α_i are experimentally determined material parameters and N is the number of model order.

It should be noted that the neo-Hookean and Gent models are generally recognized as physical-based models due to the fact that the model parameters have physical meaning for the materials. However, the Ogden model is a type of phenomenal model since the model parameters without the exact physical meaning can be determined just with the experimental data. In applications, the Ogden model usually gives a superior prediction of the response of DEAs compared to the neo-Hookean model and Gent model. Therefore, the Ogden model is also widely utilized to analyze the behaviors of DEAs [53, 72, 85–90].

3.5. Considering the viscoelasticity

In the above models based on the principles of equilibrium thermodynamics, the actuation processes of the DEAs are assumed to be without energy dissipation. However, in fact, the dielectric elastomers possess the viscoelasticity behavior, which exhibits distinctly inelastic behavior or dissipative behavior, exemplified by the creep, hysteresis, Mullins effect, and frequency-dependent responses. Viscoelasticity of course influences the actuation performance of DEAs [41, 51, 91–95]. Therefore, it has to be accounted for in the modeling in order to understand the complete electromechanical behavior of DEAs.

To deal with this problem, Suo and colleagues provided an interpretation within the nonequilibrium thermodynamics framework, that is, thermodynamics requires that the increase of the free energy δF of the elastomer membrane should not exceed the total work done by the mechanical forces $P_1\delta l_1 + P_2\delta l_2 + P_3\delta l_3$ and the work done by the battery $\Phi\delta Q$, satisfying,

$$\delta F \leqslant P_1\delta l_1 + P_2\delta l_2 + P_3\delta l_3 + \Phi\delta Q. \tag{26}$$

According to the definition of the density of the free energy W in (5), we can obtain

$$\delta W \leqslant (\sigma_1 + ED)\lambda_2\lambda_3\delta\lambda_1 + (\sigma_2 + ED)\lambda_1\lambda_3\delta\lambda_2 + \sigma_3\lambda_1\lambda_2\delta\lambda_3 + \lambda_1\lambda_2\lambda_3 E\delta D. \tag{27}$$

In the model of ideal dielectric elastomers, the stretching and polarization of the elastomer contribute to the free energy independently. Following the steps involving in the framework of equilibrium thermodynamics and the two assumptions (A1) and (A2) on ideal dielectric elastomers in section 3.3.1, the density of the Helmholtz free energy W can be described as a function of a set of independent variables

$$W(\lambda_1, \lambda_2, D, \xi_\alpha, \xi_\beta, \ldots) = W_{\text{stretch}}(\lambda_1, \lambda_2, \xi_\alpha, \xi_\beta, \ldots) + \frac{D^2}{2\varepsilon}, \tag{28}$$

where $\xi_\alpha, \xi_\beta, \ldots$ represent a set of internal variables that characterize the time-dependent nonlinear effects in the dielectric elastomer; W_{stretch} is the Helmholtz free energy associated with the stretching of the elastomer.

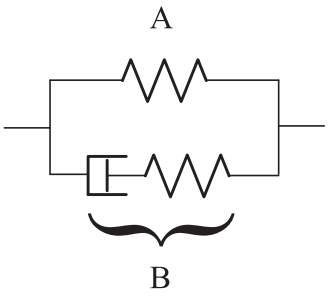

Figure 3. Schematic representation of an one-dimensional two-unit rheological model.

A combination of (27) and (28) gives that,

$$\left(\frac{\partial W}{\partial \lambda_1} - (\sigma_1 + DE)\lambda_2\lambda_3\right)\delta\lambda_1 + \left(\frac{\partial W}{\partial \lambda_2} - (\sigma_2 + DE)\lambda_1\lambda_3\right) \times \delta\lambda_2 + \left(\frac{\partial W}{\partial \lambda_3} - \sigma_3\lambda_1\lambda_2\right)\delta\lambda_3 + \left(\frac{\partial W}{\partial D} - E\right)\delta D + \sum_\gamma \frac{\partial W_{\text{stretch}}}{\partial \xi_\gamma}\delta\xi_\gamma \leqslant 0. \tag{29}$$

As pointed out in [34, 41], this inequality (29) can be satisfied in many ways. Firstly, it can be assumed that the membrane is in mechanical and electrostatic equilibrium, so that the coefficients in front of $\delta\lambda_1$, $\delta\lambda_2$, $\delta\lambda_3$ and δD vanish, such that,

$$\sigma_1 - \sigma_3 = \lambda_1\frac{\partial W_{\text{stretch}}(\lambda_1, \lambda_2, \xi_\alpha, \xi_\beta, \ldots)}{\partial\lambda_1} - \varepsilon E^2, \tag{30}$$

$$\sigma_2 - \sigma_3 = \lambda_2\frac{\partial W_{\text{stretch}}(\lambda_1, \lambda_2, \xi_\alpha, \xi_\beta, \ldots)}{\partial\lambda_2} - \varepsilon E^2 \ . \tag{31}$$

The above equations confirm a widely used description of electromechanical interaction as well, that is, the voltage produces a Maxwell stress of εE^2 as addressed in the Pelrine's approach (section 3.1).

Then, the nonlinear deviation, caused by the viscoelasticity, from the equilibrium state in the inequality (29) takes the form of,

$$\sum_\gamma \frac{\partial W_{\text{stretch}}(\lambda_1, \lambda_2, \xi_\alpha, \xi_\beta, \ldots)}{\partial\xi_\gamma}\delta\xi_\gamma \leqslant 0. \tag{32}$$

To account for the thermodynamic inequality (32), an one-dimensional rheological model of springs and dashpots with two parallel units as shown in figure 3 is generally used, where the unit A consists of an elastic spring, and the unit B consists of an elastic spring, and a linear dashpot. Then, the elastic material models as discussed in section 3.4 can be used to describe the elastic springs. For a detailed discussions of this rheological model may refer to [41, 42, 81, 94, 95]. It should be noted that modeling of the viscoelasticity is still an open task in the field of DEAs.

3.6. Considering the dynamics behaviors

Most of previous studies have focused on the quasi-static behavior of large-deformation DEAs, with the effect of inertia and damping neglected. However, it has been appreciated that DEAs can deform over a wide range of frequencies. Modeling the dynamic behaviors of the DEAs is another important and challenging task if DEAs are used in the field of soft robotics.

Recently, a few researchers have started to make the attempts to address the dynamic responses of DEAs. Based on the framework of equilibrium thermodynamics, Zhu *et al* [96] developed an analytical model to analyze the resonant behavior of a DEA, where a membrane of a dielectric elastomer was prestretched and mounted on a rigid circular ring. They demonstrated that the natural frequencies could be tuned by varying the prestretch, pressure and voltage. Similarly, Li *et al* [79] developed an analytical dynamic model for an one-dimensional in-plane DEA, where a membrane of a dielectric elastomer was prestretched and mounted on a rigid frame. They showed that prestretches and applied static voltages could tune the natural frequency and modify the dynamic behavior of the DEA. Based on the Euler–Bernoulli beam model, Feng *et al* [97] developed an analytical model to analyze the dynamic characteristics of a dielectric elastomer based microbeam resonator, in terms of the quality factor (Q-factor) and frequency shift ratio. This analytical model was validated to be applicable for a certain range of ambient pressure and active frequency tuning of the resonator could be realized by increasing the applied electrical voltage within a certain range avoiding the mechanical instability. According to the Euler–Lagrange equations, Xu *et al* [98] provided an alternative method to analyze the dynamic analysis of a homogeneously deformed DEA and extensive works have then been reported in [72, 99, 100].

It can be concluded that investigation of the dynamic behaviors of the DEAs has attracted the research attention in the society. The reported works [72, 96–100] mainly focus on the simulation results only with the analysis of the resonant behavior. However, little attention has been paid to the response speed of the DEAs, neither the response under cyclic loading-unloading voltages. In fact, most of the practical applications require actuators capable of changing deformations quickly and repeatably. In [101], Kaal and Herold investigated the dynamic behaviors of the DEA with the nonlinear electromechanical equation, which was further verified in experiments under a fix sinusoidal excitation. Rosset *et al* [102] also reported the interesting experimental results showing that the dynamic response of the DEAs may be extremely dependent not only on the membrane material, but also on the compliant electrodes. As an alternative, Sarban *et al* [103] introduced a fourth-order ordinary differential equation to describe the stress–strain relationship in DEAs, which was verified by the frequency bandwidth and hysteretic responses between simulation and experiments. However, the complete physical understanding of these dynamic behaviors has not been presented.

4. Applications for bioinspired and biomimetic soft robots

The unique performances of DEAs create a wide range of opportunities in the field of soft robotics among several areas: (i) new actuation mechanism and structural designs, (ii) new selections for modeling and mimicking of humans and natural animals, (iii) new applications with compliance matching for confined and unstructured spaces. In the following, we will review the reported soft robots using DEAs.

4.1. Configurations of DEAs

As addressed in section 2, the structure of the DEAs is simple with an elastomer membrane sandwiched by two compliant electrodes. It is this simple structure that makes it be fabricated in many configurations for extensive applications. Most DEAs are designed based on the area expansion of the thin elastomer membrane for actuation, however, multi-layer stacked or folded DEAs exist as well wherein actuation is through a reduction in thickness. Until now, a number of DEA configurations have been developed, including planar (in-plane, framed, bistable and diaphragm), rolled (tubular and cylindrical), bender (unimorph and bimorph), multi-layered (stacked and folded), conical, minimum-energy structured, and so on [29, 30, 104, 105]. As an illustration, figure 4 shows some representative configurations of DEAs.

Besides the actuator function, a DEA can be able to sense its own strain relying on change of the self-sensing signals in the DEA, generally known as self-sensing capability. Recently, several DEAs with different self-sensing signals have been developed, for instance, the force self-sensing signal [106], capacitive self-sensing signal [107–109], current self-sensing signal [110, 111] and combination of voltage and current self-sensing signals [112]. In this sense, close-loop control approaches can been applied for the self-sensing DEAs without the external sensors.

It should be mentioned that, in all these configurations, prestretch (or prestrain) is a common approach to improve the overall performance of DEAs. The main advantages of prestretch include:

(i) removing the electromechanical instability;

(ii) increasing the breakdown field;

(iii) improving the actuation strains and mechanical efficiency;

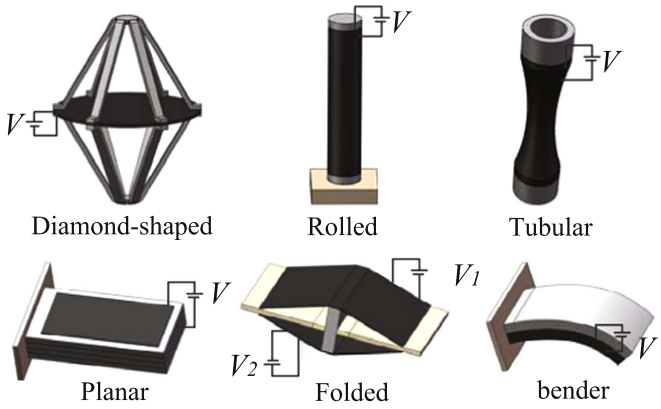

Figure 4. Representative configurations of DEAs.

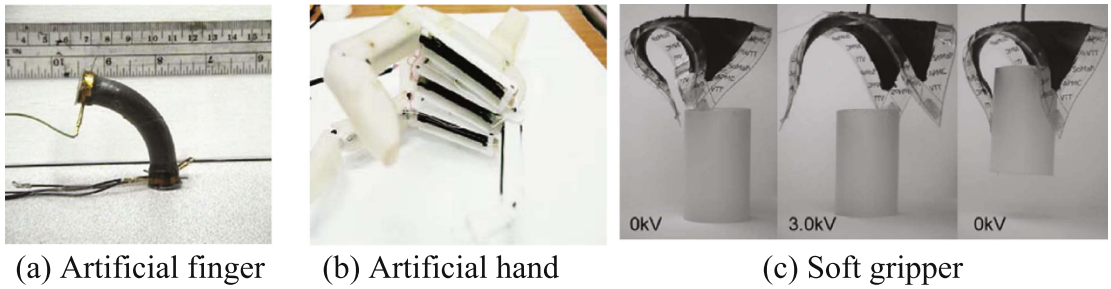

Figure 5. DEA-driven artificial muscle, finger, and hand: (a) reproduced with permission from [115], copyright 2014 IOP Publishing, (b) reproduced with permission from [116], copyright 2006 SPIE, (c) reproduced with permission from [104], copyright 2007 American Institute of Physics.

(iv) achieving preferential actuation in a certain direction.

4.2. DEA-driven soft robots

Based on different kinds of DEA configurations, researchers have developed many soft robots. These soft robots can be divided into the following categories: wearable/humanoid robots, walking/serpentine robots, flying robots and swimming robots.

4.2.1. Wearable/humanoid robots

It is the ultimate challenge to make a wearable/humanoid robot in the field of biological inspiration and mimicking, which is also known as biomimetics [113, 114]. Artificial muscles are offering important actuation capability for making such robot lifelike. As shown in figure 1, the dielectric elastomers have the closest potential to emulate natural muscles due to the similar capability of actuation strain and actuation pressure/density. Therefore, different wearable/humanoid devices or robots have been developed, generally using the antagonistic arrangement of DEAs, to mimic the function of human muscles.

In light of their biomimetic potential and growing interest in the society of soft robotics, DEAs are promising with regards to prosthetic applications [118]. The rolled DEAs usually with spring and core show promising potentials for soft robotic and prosthetic mechanisms wherever simple linear motion or bending motion is required. In general, rolled DEAs have been reported to produce up to 30 N of force, linear displacements (strokes) up to about 2 cm, cyclic speeds of more than 50 Hz, and bending angles up to 90° [115, 119]. This kind of rolled DEAs can be used to mimic the muscle of humans as illustrated in figure 5(a). Bending and gripping are simple and important mechanisms of human hands. Using rolled DEAs, a prosthetic robotic hand [116] was developed as shown in figure 5(b). This robotic hand utilized an antagonistic actuator arrangement structure and pulley system, providing each finger with 15–30 DOFs. Using a planar DEA, a three-finger gripper with a minimum energy structure was designed [104]. In this design, a passive elastic frame was combined with the prestretched elastomer such that the the energy released from the contracting elastomer could be partially stored as bending energy in the frame. As shown in figure 5(c), the three fingers were closed at rest. When a voltage of 3 kV was applied, the thickness of the elastomer reduced, and the area expanded, resulting in an opening of the three fingers. When removing the voltage, the three fingers grasped the object.

To mimic the human arms, an arm wrestling robot (figure 6) [117] was developed by using rolled DEAs,. In this robot, more than 250 DEAs with small diameters were arranged in two groups according to the

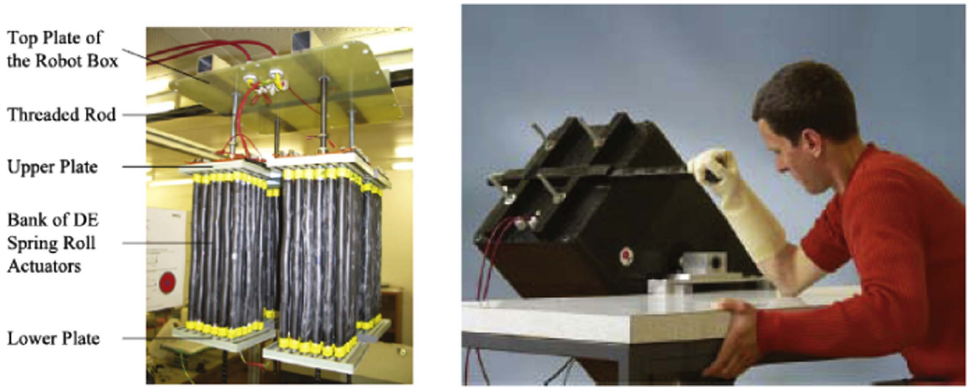

Figure 6. An arm wrestling robot made of rolled DEAs, reproduced with permission from [117], copyright 2007 IOP Publishing. Left photo: the four actuator banks, each equipped with 64 DEAs, placed inside the arm wrestling robot; right photo: wrestling match against a human arm around the rotational axis upon the table.

human agonist-antagonist muscle configuration in order to achieve an arm-like bidirectional rotation movement. They stated that the time required for the full actuation of the robot was within one second, and the robotic arm could not generate the necessary force to move back into the upright position due to the in-line arranged force transmission set-up once losing position, During the arm wrestling contest against a human arm in the 2005 EAP arm-wrestling contest, this wrestling robot lost. However, the DEAs demonstrate very promising performance as artificial muscles. As of 2006, the contest was turned to measuring the arms capability and comparing the data of the competing arms [120]. A robotic arm designed by Virginia Tech lifted a weight of 0.9 N with a height of 22 cm in approximately 4 min, yielding a force and speed capacity of less than 1% of the baseline human measurement [118]. Recently, the challenges and opportunities using DEAs for prosthetics have also been discussed in [118, 121].

Tactile sensing capability is crucial to make robots capable of safe interaction with humans or obstacles in the unstructured environments. Many researches have been made on the development of wearable devices with tactile display using DEAs. In [122], Carpi *et al* developed a wearable tactile display to provide users with tactile feedback during electronic navigation in virtual environments. The display consisted of bubble-like hydrostatically coupled DEAs (HCDEAs) was integrated within a plastic case, so that the passive elastomer membrane was in contact with the finger, while the active elastomer membrane was protected by a plastic chamber as shown in figure 7(a). They demonstrated that the converter may safely work at low maximum electrical power (less than 1 W) and the user may never be exposed to high voltage parts of the device. In this paper, they also showed that the HCDEAs were capable of utilization for dynamic Braille displays and for finger rehabilitation. Lee *et al* [123] presented a multiply arrayed tactile display device with DEAs. The device employed the liquid coupling between the touch spot and the actuator as the transmission of force as shown in figure 7(b). They demonstrated that the force was over 40 mN to stimulate the human finger tip and the displacements of tactile display were about 240–120 μm at 3–10 Hz, which may satisfy the frequency requirements for stimulating the Merkel cells as well as the Meissner corpuscles. Alternatively, based on the knowledge that humans are very sensitive to shear force distributions, Knoop and Rossiter [124] developed a new DEA-actuated shear tactile display device as shown in figure 7(c). They demonstrated that this device allowed for the areal expansion of the DEA to be exploited directly, and a tactile display could be made with no elements moving out of the plane.

The visual system is another important part of humanoid robots for focusing and tracking. Researchers have presented some attempts to mimic the eyeball muscle system of humans with DEAs. As shown in figure 8(a) , Carpi and De Rossi [125] developed bioinspired pseudomuscular eyeballs using a contractile DEA for an android robotic face. The arrangement and the functionality of the actuators were conceived to mimic the rectus-type human ocular muscles. DEA-driven eyeball was shown to rotate up to approximately $\pm 25°$. They [128] also developed a new mechanism of actuation of a robotic eyeball using a buckling DEA with constrained boundaries, which could obtain a maximum displacement higher than 70% of the pre-curvature height. As an alternative, Liu *et al* [126] developed a mechanism (figure 8(b)) with an inflated DEA to mimic the ocular muscle of the human eye. They demonstrated that the inflated DEA, compared with uninflated one, performed much bigger rotating angle and more strengthened. Recently, a more interesting biomimetic lens (figure 9) inspired by the architecture of the crystalline lens and ciliary muscle of the human eye was reported in [127]. It consisted of a fluid-filled elastomeric lens integrated with an annular DEA working as an artificial muscle. The experiments demonstrated that the artificial lens

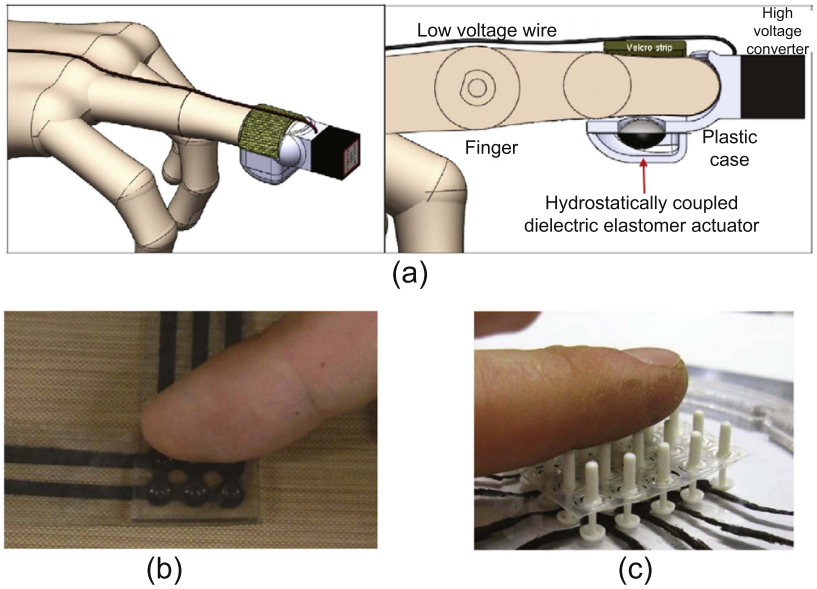

Figure 7. Wearable/tactile devices made of DEAs: (a) reproduced with permission from [122], copyright 2011 SPIE, (b) reproduced with permission from [123], copyright 2014 Elsevier, (c) reproduced with permission from [124], copyright 2014 SPIE.

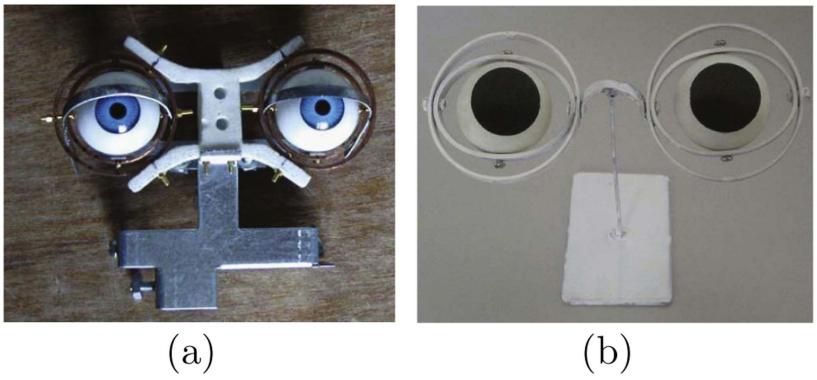

Figure 8. Mechanism of pseudomuscular eyeballs using DEAs: (a) reproduced with permission from [125], copyright 2005 SPIE; (b) reproduced with permission from [126], copyright 2008 SPIE.

showed dynamic properties suitable for operation at a maximum frequency of 1–10 Hz and the response to the step stimulus had a time constant (time to reach 63.2% of the asymptotic value) $\tau \cong 60$ ms.

4.2.2. Walking/serpentine robots

In 2001, Eckerle *et al* [132] developed and reported a first kind of DEA-driven biomimetic walking robot, named as FLEX, with six legs. FLEX had a weight of 670 g and used dielectric elastomer acrylic bowtie actuators, with two degrees of freedom per leg (up/down and forward/back). They demonstrated that FLEX could walk at the speed of a few millimeters per second. However, the speed of this robot is too slow. In 2002, an improved six-legged walking robot [129], known as FLEX 2, was developed by the same group based on the same basic kinematic design of FLEX. FLEX 2 used a more powerful rolled DEAs as shown in figure 10(a). The walking speed of FLEX 2 was demonstrated to increase from an unimpressive few millimeters per second to a respectable 3.5 cm s^{-1} and lifetime and shelf life were dramatically improved as well. It should be noted that both FLEX and FLEX 2 are autonomous, containing a battery-powered device that included voltage conversion and microprocessor controller on board. The series of FLEX robots can be recognized as a milestone in the field of DEA-driven biomimetic robots.

As a further step, Pei *et al* [115, 130] designed another two kinds of DEA-driven walking robots, named as Skitter and MERbot, respectively. Skitter was a small, legged robot as shown in figure 10(b), which used six single-degree-of-freedom rolled DEA to provide six legs. Skitter was demonstrated to reach a peak speed of approximately 7 cm s^{-1}. Alternatively, MERbot was a novel six-legged robot with six 2-DOF rolled DEAs as legs as shown in figure 10(c). MERbot had the dimensions of 18 cm $\times$18 cm $\times$10 cm, and

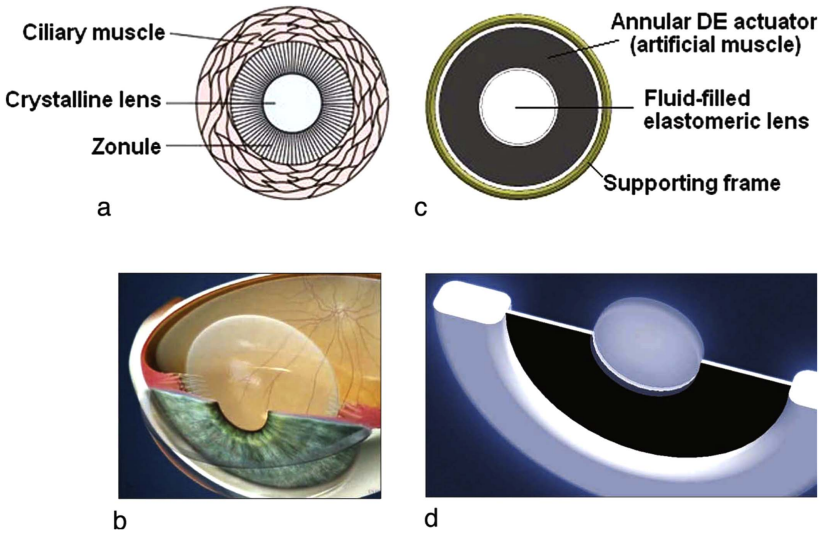

Figure 9. Morphological comparison between the human lens and the biomimitic lens using DEAs reproduced with permission from [127], copyright 2011 Wiley.

had the weight of 292 g. MERbot could walk with a dual tripod gait. Experiments demonstrated that the maximum speed of the MERbot could be up to 13.6 cm s^{-1} at 7 Hz and 5.5 kV, which was equivalent to roughly two-thirds of its body length per second.

Alternatively, Nguyen and colleagues [131] developed a small biomimetic quadruped robot driven by multistacked DEAs as shown in figure 10(d). Each leg of the quadruped robot contained two DEAs to achieve the motion of a swing phase and a stance phase. The total size of the robot was 191mm $\times$100 mm $\times$115 mm and the total weight was 450 g. Experimental results demonstrated that the robot's legs could perform walking gaits as well as running gaits. Recently, they also developed a printable hexapod robot driven by the multi-DOF conical DEAs [133]. To achieve alternating tripod gaits of the hexapod robot, a sequence of legs motions were defined, i.e., (a) passive state, (b) lifting upward, (c) swinging forward, (d) pushing downward and (e) swinging backward. The experimental results showed that the robot obtained the walking speed of 4 mm s^{-1} when the square wave voltage of 3.5 kV was applied to the DEAs with the frequency of 0.5 Hz.

Different from the legged robots with the DEAs in parallel, the snake-like serpentine robots can be developed with the bending rolled DEAs in series with a monolithic structure. With this idea, a proof-of-concept serpentine robot was developed in [115]. This snake-like roboth had four segmented DEAs in series as shown in figure 11(a). Each segment could be individually actuated like a single 2-DOF actuator. Hence, this robot had a total 8-DOFs in two groups, *LRLRLR* and *RLRLRL*, where *L* meaned a left circumferential span and *R* means a right span. Experiments showed that the two groups were actuated successively at 6 kV to generate a serpentine motion.

Similarly, a annelid-like earthworm robot (figure 11(b)) was reported in [134]. This robot had two sectors in terms of front and rear, and each sector had four actuator modules. A 3-DOF motion, i.e., up-down translational motion, and two rotational, could be presented. They demonstrated that the speed of the earthworm robot relied on the operating frequency of each actuator. Experimental results showed that the robot had a speed of about 1 mm s^{-1} with 5 Hz actuation.

Using unimorph DEAs, Shian *et al* [135] presented a proof-of-concept inchworm robot as shown in figure 11(c). In this robot, a few aligned fibers were incorporated to suppress undesirable actuator bulging and more effectively convert the bending of the DEA to forward motion. They demonstrated that after adding four fibers of larger diameter, the bending curvature increased and the forward speed improved. The experimental results also showed that at each cycle, the inchworm robot moved at approximately 3.8 mm. When at 0.3 Hz actuation rate, the average speed of the robot was 1.1 mm s^{-1}, which corresponded to length-specific speed of 1.3 body lengths per minute.

As an alternative, Petralia and Wood [136] presented another kind of snake-like robot with 5 DEA-based minimum-energy structures (termed as DEMS). The experimental results demonstrated that the serpentine robot experienced a 1.7 times increase in length and a 1.4 times decrease in height upon application of 1.2 kV to all ten segments.

4.2.3. Flying robots

The design of flying robots with flapping wings is usually inspired from the flying insects whose wings are driven indirectly by muscles located in their thoraxes. The DEAs are selected as a potential

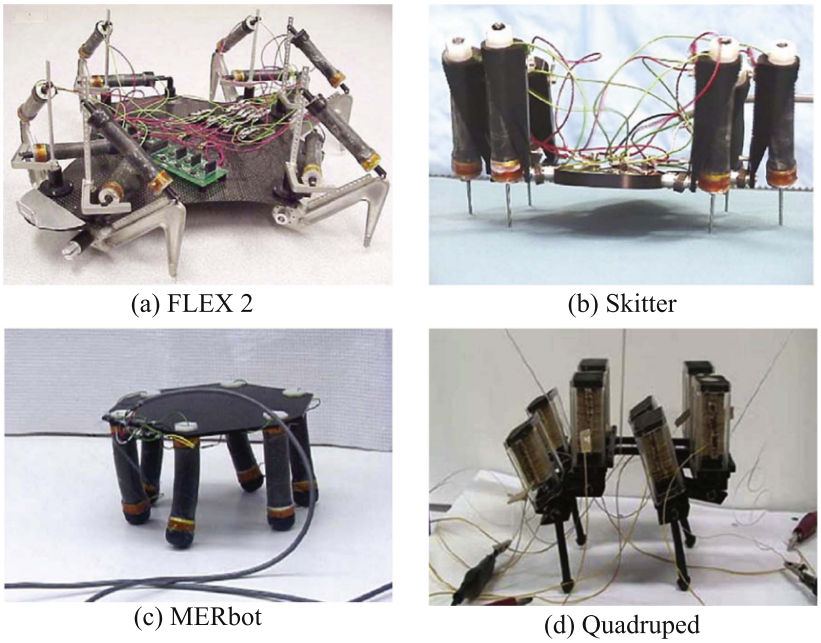

Figure 10. DEA-driven walking robots: (a) reproduced with permission from [129], copyright 2002 SPIE, (b) reproduced with permission from [130], copyright 2002 SPIE, (c) reproduced with permission from [115], copyright 2004 IOP Publishing, (d) reproduced with permission from [131], copyright 2014 IOP Publishing.

actuation technology mainly due to their capabilities of high actuation density and large strain with higher speed.

SRI researchers from America [38, 129] in 2002 started to develop a flapping-wing mechanism using a stack DEA. By studying the behaviors of flying insects, they found that the muscles of the insects flexed the exoskeleton and moved the wings, which were attached to the exoskeleton. In the same way, the stack DEA could be used as a bundle of artificial muscles, which flexed a plastic exoskeleton with the attached wings. Based on this idea, a flying robot was designed as shown in figure 12(a). However, they demonstrated that the work density of the flying robot became dramatically lower in experiments, which may be caused by the high passive weight of the supported structure and its integration with the DEA. Therefore, further development needs to be made in order to reach desired power densities for the entire robot.

In [137], a bioinspired flapping wing robot as shown in figure 12(b) was developed by a group in NTU, Singapore, with a rolled DEA and lightweight carbon fiber reinforced polymer (CFRP) shell. This DEA assembly using the CFRP shell was demonstrated to achieve 30.9% of the theoretical work density for a BJB-TC5005 membrane at 33.5 MV m^{-1}. The flapping robot had a total weight of 10.47 g, of which 50% was due to the DEA, 17.4% was due to the CFRP shell, and 17.8% was due to the thoracic mechanism. Each wing of the robot had the size of 6 cm long and 0.16 g weight. Experiments showed that wings flapped with a mere 5°–10° stroke at the frequency of 1 Hz.

Inspired by the 'jumping' of the creatures such as kangaroos, fleas or grasshoppers, hopping robots using DEAs were developed by the research groups of SRI [138] and MIT [139]. These robots are generally simple and lightweight and have an energy storage mechanism to mimic the capabilities of jumping many times their body height, which can thereby overcome the uneven terrain. By using three flat film DEAs in a tripod configuration, a hopping robot [138] (figure 12(c)) was designed with the dimensions of 5.5 cm ×5.5 cm ×1.5 cm, which could jump approximately 2 cm vertically, about 1.33 times its body height. By combining the diamond shaped DEAs with the bistable mechanism, Plante in his thesis [139] developed a millimeter-scale hopping robot. This kind of novel bistable mechanism allowed DEAs to provide intermittent motion, an essential condition for their reliability. Experimental results demonstrated that, with the total cycle time of about 20 s, the hopping robot can jump up to the height of almost 10 cm. The next development of hopping robots may integrate both the waling and jumping capabilities together, which are more biomimetic like natural animals, locomotion on both smooth and uneven terrains.

A more interesting work on a flying robot was recently reported by Shea's group from EPFL, Switzerland [140]. In their work, the foldable antagonistic DEA with outline size of 70 mm ×130 mm was developed as elevons to control flight surfaces of a fixed wing UAV with the angular displacement range and the torque specification matched to a 400 mm wingspan micro-air vehicle of mass 130 g. They

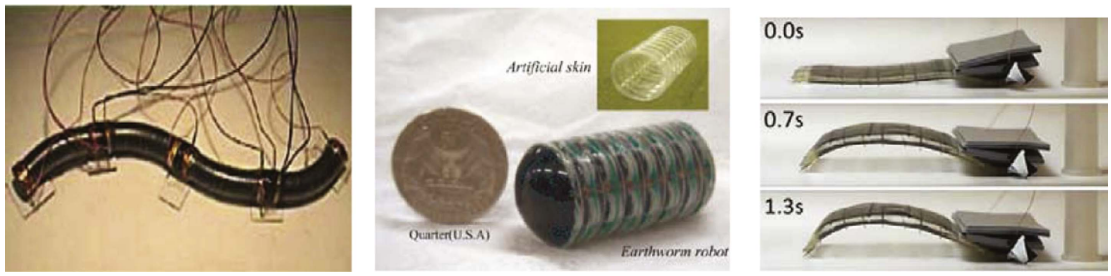

Figure 11. DEA-driven serpentine robots: (a) reproduced with permission from [115], copyright 2004 IOP Publishing, (b) reproduced with permission from [134] copyright 2007 IOP Publishing, (c) reproduced with permission from [135], copyright 2015 SPIE.

demonstrated voltage-controllable angular displacement up to $\pm 26^{\circ}$ and torque of 2720 mN mm at 5 kV.

4.2.4. Swimming robots

Generally, development of bioinspired and biomimetic swimming robots using DEAs is attractive because the density of the dielectric elastomers approximately equal to that of water, which makes them as a desired choice for keeping neutral buoyancy. In fact, most realistic underwater swimming robots operate with neutral buoyancy. Otherwise, a significant amount of power will be consumed by maintaining equilibrium of the robots under water. However, until now, little work has been reported to develop biomimetic swimming robots using DEAs.

In [141], Laschi *et al* provided a concept of designing a swimming robot inspired by the octopus arm using DEAs. However, the real robot is not presented in this work.

As a more recent progress [142], Godaba and the colleagues developed a jellyfish robot using a DEA. Experimental results demonstrated that the jellyfish robot had the weight of 256 g and could be able to achieve a payload of 236 g, compared to its self-weight. Experimental results demonstrated that the maximum velocity attained by the jellyfish robot was around 0.3 body length per second.

5. Summary and outlook

From the aforementioned survey and discussions, we can conclude that DEAs are becoming more and more promising for the rapid development of soft robotics with the features of bioinspiration and biomimetics. In the last decade, the researchers have made extensive efforts in this research field. However, there is still a long way to go to completely understand the electromechanical and physical behaviors of DEAs, design and control the soft robots like the natural soft bodied animals, which needs to be tackled together by the researchers from different subjects.

At the end of this paper, we will summarize the main challenges and opportunities on the DEA-driven soft robots for further studies from the following three aspects: design, modeling and control.

5.1. Design

The concept of taking inspiration from soft-bodied animals can provide invaluable insights for the continuous development of soft robots. Design of novel durable structures and mechanisms with multi-degree of freedom is still the major way to achieve bioinspried and biomimetic capabilities or intelligence, which can be possible with the development of new DEAs. For instance, there is still significant room for improvement of materials to meet industrial requirements regarding lifetime and fault-tolerance, which are essential for applications in actual soft robots or devices. Invention of new kind of dielectric elastomers with higher dielectric constants and material strengths may further increase the performance of the actuators. It should be mentioned that actuator design should not focus only on achieving the maximum attainable strain, but also on enhancing the specific performance within a reliable operating range. Besides, exploring of more diverse compliant electrodes with the new characteristics of transparency, tunable color or camouflage can firmly broaden the applications of DEAs.

It should be noted that, during the past decades, it is more common to use other kinds of soft materials [11, 143–146], such as the SMAs, ionic polymer-metal composites and pneumatic muscles, for biomimetic applications. Recently, dielectric elastomer materials become promising in the emerging field of soft robotics due to the advantages of voltage-induced deformation, light weight, high deformation, high energy density, and fast response. One main concern about the DEAs may be its electrical safety because the very high voltage (usually more than 1 kV) is required to drive the DEAs. However, the required current is generally small (on the order of 10^{-6} A). According to the discussion in [147], a general phrase on electrical safety says that it is not voltage that kills, but current. For example, a current less than 1 mA may not limit ones perception [147]. As a result, the DEA is safe due to its low current, and the electric safety can be

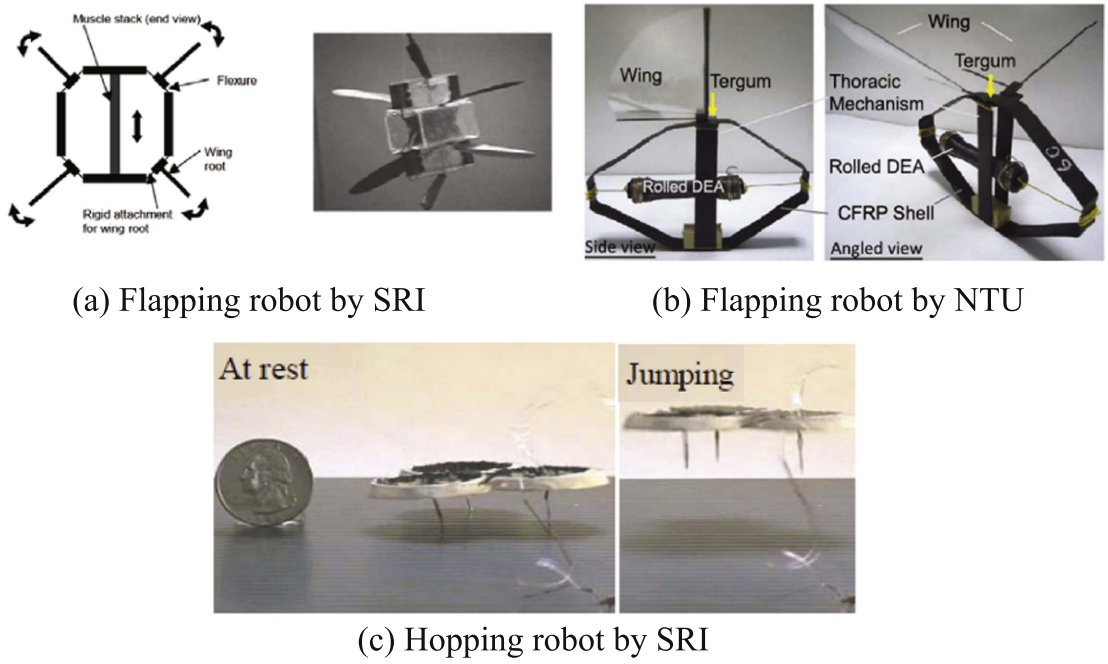

Figure 12. Flying robots using DEAs. (a) reproduced with permission from [38], copyright 2002 SPIE, (b) reproduced with permission from [137], copyright 2014 IOP Publishing, (c) reproduced with permission from [138], copyright 2004 SPIE.

ensured when the high-voltage parts are insulated from the user. In real applications, it is worth noting that the first mass-produced application of dielectric elastomer technology has been for a wearable system (a vibrating haptic-feedback device for a gaming headset) and it uses high voltages [148]. In [149], dielectric elastomers are also being explored extensively for biomedical applications. In order to boost DEAs for industrial exploitation, other technologies are also investigated to drive the DEAs with lower voltage. One main task as pointed out by Carpi *et al* [122] may be to find a kind of new elastomer films that can be driven at lower voltages, for instance, the possibility of ideally driving DEAs at the same voltage range of piezoelectric actuators. As an early attempt, decreasing the thickness of the membrane in DEAs may be another possible choice. For instance, by introducing a spin coating technique, fully automated fabrication of DEAs with layer thickness down to 5 μm and actuator diameter up to 40 mm was reported, which thus enabled the driving voltages of DEAs far below 1 kV [150].

Another challenge on design is that most of DEAs are fabricated by hand. As an early and important attempt, Lotz and colleagues [150] provided a fully automated fabrication process to produce a stacked DEA with four steps: (i) two components of uncured polydimethylsiloxane (PDMS) are mixed and applied onto the disk of a spin coater; (ii) heating accelerates the curing process of the PDMS; (iii) graphite powder is sprayed onto the PDMS surface, where the electrode is patterned by the use of a shadow mask; (iv) repeating steps (i)–(iii) to build stacked layers for up to 100 times. Typically, a single layer is fabricated within 5 min. Recently, Araromi and colleagues [151] developed a novel fabrication methodology for high-resolution patterning of compliant electrodes for stretchable dielectric elastomer actuators and sensors with PDMS. This approach employed cast PDMS-carbon electrodes patterned by laser ablation and achieved robust permanent bonding to a silicone elastomer membrane by oxygen plasma activation. The generalized fabrication methodology was outlined in figure 13. A variety of transducer designs with sub-200 μm feature sizes over large areas (over 100 cm^2) were demonstrated to be fabricated using this approach. As discussed in section 4.1, prestretch is necessary in fabrication of DEAs. Alternatively, Duduta *et al* [152] proposed a combination of materials and multilayer fabrication method without prestrech. With the rapid development of additive manufacturing, the new innovation in soft lithography, 3D printing, and other rapid prototyping technologies shall open the way to batch produce commercial soft robots with DEAs that are inexpensive and meet the commercial demand.

In addition, the soft robots using DEAs are usually designed to function with voltage supplied through an external driver tether. Although this tether may interfere with some tasks, such as ease of control and long-time work without battery, it is often an advantage rather than a disadvantage. Nonetheless, robots intended for use outside of laboratory environments are required to be able to operate without the constraints of a tether, especially when robots are intended to perform tasks in confined spaces or challenging environments [25]. We should mention that with a small voltage amplifier (saying, EMCO product), the DEA can also be powered by a low voltage battery. In this

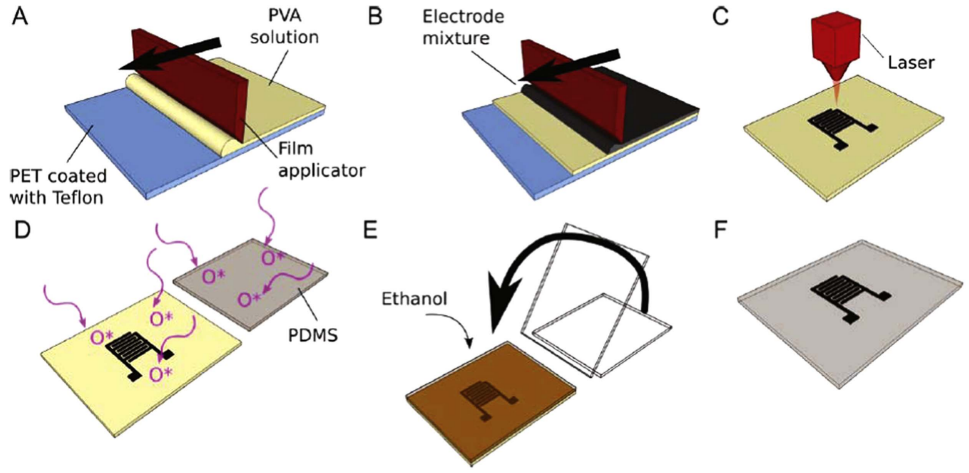

Figure 13. Automated fabrication approaches for DEAs with PDMS by laser ablation and oxygen plasma activation reproduced with permission from [151], copyright 2015 American Chemical Society.

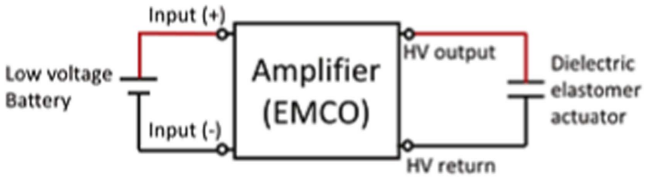

Figure 14. Schematic of on-board power system for a DEA.

way, all the power supply can be assembled on-board due to their small volume and the small weight. The main reason for use of on-board power supply is that the DEA requires high voltage (10^3 V), low current (10^{-6} A) and low power (10^{-3} W). The high voltage can be supplied by the voltage amplifier, and the low power allows for the low-voltage battery and low-sized voltage amplifier. Figure 14 shows a schematic of the power system, which consists of the microcontroller, the low-voltage battery, and the high voltage amplifier (saying the EMCO product). In our current experiments, the high voltage amplifier, saying EMCO Q101, has a size of 10 cm^3 and a weight of 28 g. The voltage amplifier can output high voltage of 10 kV. However, it should be noted that the motion performance of DEAs with the on-board amplifier (such as the EMCO product) cannot reach the same level as with an external tethered amplifier (saying the Trek product) based on our experimental results. Recently, some researchers [153–155] have also been started to design the custom-built circuits for dielectric elastomer based devices. Development of the autonomous DEA-driven soft robots is of course an interesting topic in the near future.

5.2. Modeling

The dielectric elastomers are highly nonlinear materials, which often show changeable stiffness and complex dynamics when rapidly stretched, display creep under constant loads, and exhibit Mullins effect and hysteresis upon cyclic loading. Therefore, the mechanical responses of DEAs and DEA-driven robots are strong nonlinear, time-dependent and frequency-dependent. There has been a great progress on electromechanical modeling of DEAs, especially the development based on the continuum mechanics and thermodynamics to understand the electromechanical instability and electrical breakdown. However, few works are reported to account for the viscoelasticity, hysteresis and vibrational dynamics with experimental explanations. Maximum strain before breakdown, hysteresis in the voltage–displacement relation, toughness and fatigue are needed to be better understood in the near future. These time and history dependent responses not only make modeling challenging, they also require distributed sensory feedback in the practical design of soft robots [37].

5.3. Control

Compared to the diverse achievements on design and modeling, few efforts have been made in the area of control of DEAs and DEA-driven robots. Although some works were reported to control DEAs with adaptive [157–159], or feedback [108] techniques, the nonlinear material behavior, viscoelasticity and hysteretic effects were generally ignored in their development. As a result, these approaches are generally effective for small displacement, or able to control

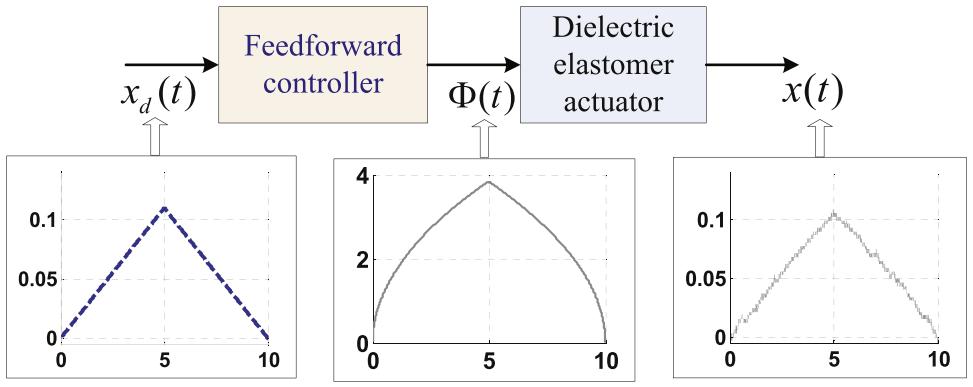

Figure 15. Block diagram of the feedforward deformation controller: $x_d(t)$ represents the desired trajectory, $\Phi(t)$ represents the control voltage generated by the feedforward controller, $x(t)$ represents the deformation of the actuator, reproduced with permission from [156], copyright 2015 American Institute of Physics.

displacement for short periods. The control challenge of the soft robots using the DEAs may be mainly due to the inherent large-deformation nonlinearities in the system, such as soft dynamics, electromechanical instability, viscoelasticity and hysteresis.

To tackle this challenge, feedforward control with a solid nonlinear dynamic model may be one promising approach, which is schematically shown in figure 15. In [156], Gu *et al* underlined the importance of a nonlinear dynamic model as the basis for feedforward deformation control of a rubber-based DEA, which was verified by the experimental results. This work confirms that a DEAs trajectory can be finely controlled with a solid nonlinear dynamic model despite the presence of material nonlinearities and electromechanical coupling. Different from the physical-based modeling approach, a phenomenological model based feedforward control approach was proposed for both the creep and vibration compensation of a circular DEA [160]. The experimental results demonstrated that the creep of the DEA was reduced from 20% into less than 7%, and the overshoot initially about 38.72% was almost completely removed. With the development of the transfer function models taking into account the viscoelastic effect, Nguyen *et al* [161] developed an inversion-based feedforward controller for sensorless position control of the DEAs and the parallel-crank mechanism articulated with these actuators. Experimental results were also conducted in this work to well demonstrate effectiveness of the proposed control approach. As an alternative, a recent work on PID feedback control were presented in [56]. However, from the experiments and discussions, the developed PID controller could only be used for the specific step signal with the constant input voltage, and loop-shaping H_∞ robust controller was not effective for tracking the sinusoidal signal. Although there are some drawbacks in this work, it is a positive early attempt to develop feedback controllers for the DEA with experimental verifications.

The postponement of control design may be due to the following reasons: (i) the complete understanding of the nonlinear dynamic behaviors of the DEAs with a general model is not available; (ii) the well-known control theories and techniques for the conventional industrial robots are poorly applicable for the soft robots with DEAs; (iii) the progress on DEAs and soft robots using DEAs have mainly been accomplished by the researchers in the fields of materials, mechanics and physics. Therefore, the developed soft robots are generally reported to have the ability of quantitative performance, while lack of accuracy analysis. With the next development of DEA-driven soft robots, the multidisciplinary integration of materials, mechanics, physics and robotics will open new perspectives for control design of soft robots. As indicated in [10, 19, 162], the concepts of self-organization, embodied intelligence, such as neural network and fuzzy system, and morphological computation may potentially be used to control soft robots in the near future. On the other hand, due to the continuum deformation nature of the DEAs, there are infinite DOF of soft robots. However, the number of the control variables is finite, which is similar to the under-actuated robots. Therefore, the control efforts and achievements of the under-actuated robotic systems [163, 164] may also be taken into account for the control design of the soft robotic systems using DEAs.

5.4. Challenges for robotic applications

From the literature survey, many kinds of DEA-based robots have been designed and developed with the bioinspired and biomimetic behaviors in the past decade. However, there are still big gaps between the developed robots and real biological examples. For instance, (i) how to design and develop the soft robots that are really ready for field applications with the capabilities of stability, robust and agility is still a challenge; (ii) rather than the conventional industrial robots, there is still no a standard or general tool to develop a kind of soft robot using DEAs. Until now,

the development relies on the experiences of the researchers; (iii) the high voltage is still a potential challenge for the applications interacting with humans. On the other hand, these challenges also represent the exciting and promising opportunities for the scientists and multidisciplinary integrations are required to create a new generation of soft robots that can be used in the real world.

Acknowledgments

The authors would like to thank H Godaba and U Gupta from National University of Singapore for their valuable discussions and suggestions. This work was in part supported by the National Natural Science Foundation of China under Grant Nos. 51622506 and 51620105002, and the Science and Technology Commission of Shanghai Municipality under Grant 16JC1401000.

References

[1] DuRant H and You J 2014 Humans need not apply *Science* **346** 190–1
[2] Bohannon J 2014 Meet your new co-worker *Science* **346** 180–1
[3] Marvel J, Falco J and Marstio I 2015 Characterizing task-based human-robot collaboration safety in manufacturing *IEEE Trans. Syst., Man, Cybern.: Syst.* **45** 260–75
[4] Wakamatsu H, Arai E and Hirai S 2006 Knotting/unknotting manipulation of deformable linear objects *Int. J. Robot. Res.* **25** 371–95
[5] Saha M and Isto P 2007 Manipulation planning for deformable linear objects *IEEE Trans. Robot.* **23** 1141–50
[6] Ding F, Huang J, Wang Y, Matsuno T and Fukuda T 2014 Vibration damping in manipulation of deformable linear objects using sliding mode control *Adv. Robot.* **28** 157–72
[7] Calanca A, Muradore R and Fiorini P 2016 A review of algorithms for compliant control of stiff and fixed-compliance robots *IEEE/ASME Trans. Mechatronics* **21** 613–24
[8] Albu-Schäffer A, Eiberger O, Grebenstein M, Haddadin S, Ott C, Wimböck T, Wolf S and Hirzinger G 2008 Soft robotics *IEEE Robot. Autom. Mag.* **15** 20–30
[9] Rus D and Tolley M T 2015 Design, fabrication and control of soft robots *Nature* **521** 467–75
[10] Pfeifer R, Lungarella M and Iida F 2012 The challenges ahead for bio-inspired soft robotics *Commun. ACM* **55** 76–87
[11] Kim S, Laschi C and Trimmer B 2013 Soft robotics: a bioinspired evolution in robotics *Trends Biotechnol.* **31** 287–94
[12] Majidi C 2014 Soft robotics: a perspectivecurrent trends and prospects for the future *Soft Robot.* **1** 5–11
[13] Robinson G and Davies J B C 1999 Continuum robots-a state of the art *Proc. IEEE Int. Conf. on Robotics and Automation* vol 4, pp 2849–54
[14] Webster R J III and Jones B A 2010 Design and kinematic modeling of constant curvature continuum robots: a review *Int. J. Robot. Res.* **29** 1661–83
[15] Trivedi D, Rahn C D, Kier W M and Walker I D 2008 Soft robotics: biological inspiration, state of the art, and future research *Appl. Bionics and Biomech.* **5** 99–117
[16] Zhao X 2014 Multi-scale multi-mechanism design of tough hydrogels: building dissipation into stretchy networks *Soft Matter* **10** 672–87
[17] Lin H T, Leisk G G and Trimmer B 2011 Goqbot: a caterpillar-inspired soft-bodied rolling robot *Bioinspiration Biomimetics* **6** 026007
[18] Ge Q, Dunn C K, Qi H J and Dunn M L 2014 Active origami by 4d printing *Smart Mater. Struct.* **23** 094007
[19] Laschi C and Cianchetti M 2014 Soft robotics: new perspectives for robot bodyware and control *Frontiers Bioeng. Biotechnol.* **2** 282–92
[20] Margheri L, Laschi C and Mazzolai B 2012 Soft robotic arm inspired by the octopus: I. From biological functions to artificial requirements *Bioinspiration Biomimetics* **7** 25004
[21] Mazzolai B, Margheri L, Cianchetti M, Dario P and Laschi C 2012 Soft-robotic arm inspired by the octopus: II. From artificial requirements to innovative technological solutions *Bioinspiration Biomimetics* **7** 025005
[22] Daerden F and Lefeber D 2002 Pneumatic artificial muscles: actuators for robotics and automation *Eur. J. Mech. Environ. Eng.* **47** 11–21
[23] Shepherd R F, Ilievski F, Choi W, Morin S A, Stokes A A, Mazzeo A D, Chen X, Wang M and Whitesides G M 2011 Multigait soft robot *Proc. Natl Acad. Sci.* **108** 20400–3
[24] Morin S A, Shepherd R F, Kwok S W, Stokes A A, Nemiroski A and Whitesides G M 2012 Camouflage and display for soft machines *Science* **337** 828–32
[25] Tolley M T *et al* 2014 A resilient, untethered soft robot *Soft Robot.* **1** 213–23
[26] Bar-Cohen Y 2004 *Electroactive Polymer (EAP) Actuators as Artificial Muscles: Reality, Potential, and Challenges* 2nd edn (Bellingham, WA: SPIE)
[27] Carpi F, De Rossi D, Kornbluh R, Pelrine R and Sommer-Larsen P 2008 *Dielectric Elastomers as Electromechanical Transducers: Fundamentals, Materials, Devices, Models and Applications of an Emerging Electroactive Polymer Technology* (Amsterdam: Elsevier)
[28] Carpi F, Kornbluh R, Sommer-Larsen P, De Rossi D and Alici G 2011 Introduction to the focused section on electroactive polymer mechatronics *IEEE/ASME Trans. Mechatronics* **16** 1–7
[29] Brochu P and Pei Q 2010 Advances in dielectric elastomers for actuators and artificial muscles *Macromol. Rapid Commun.* **31** 10–36
[30] Halloran A O, Malley F O and McHugh P 2008 A review on dielectric elastomer actuators, technology, applications, and challenges *J. Appl. Phys.* **104** 071101
[31] Carpi F, Bauer S and De Rossi D 2010 Stretching dielectric elastomer performance *Science* **330** 1759–61
[32] Keplinger C, Kaltenbrunner M, Arnold N and Bauer S 2010 Röntgens electrode-free elastomer actuators without electromechanical pull-in instability *Proc. Natl Acad. Sci.* **107** 4505–10
[33] Röntgen W C 1880 Ueber die durch electricität bewirkten form-und volumenänderungen von dielectrischen körpern *Ann. Phys., Lpz.* **247** 771–86
[34] Suo Z 2010 Theory of dielectric elastomers *Acta Mech. Solida Sin.* **23** 549–78
[35] Pelrine R, Kornbluh R, Pei Q and Joseph J 2000 High-speed electrically actuated elastomers with strain greater than 100% *Science* **287** 836–9
[36] Pelrine R E, Kornbluh R D and Joseph J P 1998 Electrostriction of polymer dielectrics with compliant electrodes as a means of actuation *Sensors Actuators* A **64** 77–85
[37] Bauer S, Bauer-Gogonea S, Graz I, Kaltenbrunner M, Keplinger C and Schwödiauer R 2014 25th anniversary article: a soft future: from robots and sensor skin to energy harvesters *Adv. Mater.* **26** 149–62
[38] Kornbluh R D, Pelrine R, Pei Q, Heydt R, Stanford S, Oh S and Eckerle J 2002 Electroelastomers: applications of dielectric elastomer transducers for actuation, generation, and smart structures *SPIE's 9th Annual Int. Symp. on Smart Structures and Materials* vol 4698, pp 254–70

[39] Godaba H, Foo C C, Zhang Z Q, Khoo B C and Zhu J 2014 Giant voltage-induced deformation of a dielectric elastomer under a constant pressure *Appl. Phys. Lett.* **105** 112901
[40] Li T, Keplinger C, Baumgartner R, Bauer S, Yang W and Suo Z 2013 Giant voltage-induced deformation in dielectric elastomers near the verge of snap-through instability *J. Mech. Phys. Solids* **61** 611–28
[41] Foo C C, Cai S, Koh S, Bauer S and Suo Z 2012 Model of dissipative dielectric elastomers *J. Appl. Phys.* **111** 034102
[42] Hong W 2011 Modeling viscoelastic dielectrics *J. Mech. Phys. Solids* **59** 637–50
[43] Kofod G 2001 Dielectric elastomer actuators *PhD Thesis* The Technical University of Denmark
[44] Carpi F, Chiarelli P, Mazzoldi A and De Rossi D 2003 Electromechanical characterisation of dielectric elastomer planar actuators: comparative evaluation of different electrode materials and different counterloads *Sensors Actuators* A **107** 85–95
[45] Rosset S and Shea H R 2013 Flexible and stretchable electrodes for dielectric elastomer actuators *Appl. Phys.* A **110** 281–307
[46] Low S H and Lau G K 2014 Bi-axially crumpled silver thin-film electrodes for dielectric elastomer actuators *Smart Mater. Struct.* **23** 125021
[47] Keplinger C, Sun J Y, Foo C C, Rothemund P, Whitesides G M and Suo Z 2013 Stretchable, transparent, ionic conductors *Science* **341** 984–7
[48] Kofod G, Sommer-Larsen P, Kornbluh R and Pelrine R 2003 Actuation response of polyacrylate dielectric elastomers *J. Intell. Mater. Syst. Struct.* **14** 787–93
[49] Sommer-Larsen P and Larsen A L 2004 Materials for dielectric elastomer actuators *Smart Structures and Materials* pp 68–77
[50] Kofod G and Sommer-Larsen P 2005 Silicone dielectric elastomer actuators: finite-elasticity model of actuation *Sensors Actuators* A **122** 273–83
[51] Plante J and Dubowsky S 2007 On the performance mechanisms of dielectric elastomer actuators *Sensors Actuators* A **137** 96–109
[52] Wissler M and Mazza E 2007 Electromechanical coupling in dielectric elastomer actuators *Sensors Actuators* A **138** 384–93
[53] Liu Y, Liu L, Zhang Z and Leng J 2009 Dielectric elastomer film actuators: characterization, experiment and analysis *Smart Mater. Struct.* **18** 095024
[54] Gisby T A, Xie S Q, Calius E P and Anderson I A 2010 Leakage current as a predictor of failure in dielectric elastomer actuators *SPIE Smart Structures and Materials+ Nondestructive Evaluation and Health Monitoring*764213
[55] Zhao X and Suo Z 2010 Theory of dielectric elastomers capable of giant deformation of actuation *Phys. Rev. Lett.* **104** 178302
[56] Rizzello G, Naso D, York A and Seelecke S 2015 Modeling, identification, and control of a dielectric electro-active polymer positioning system *IEEE Trans. Control Syst. Technol.* **23** 632–43
[57] Mooney M 1940 A theory of large elastic deformation *J. Appl. Phys.* **11** 582–92
[58] Rivlin R S and Sawyers K N 1971 Nonlinear continucm mechanics of viscoelastic fluids *Annu. Rev. Fluid Mech.* **3** 117–46
[59] Ogden R W 1972 Large deformation isotropic elasticity-on the correlation of theory and experiment for incompressible rubberlike solids *Proc. R. Soc.* A **326** 565–84
[60] Ronald L and Treloar G 1975 *The Physics of Rubber Elasticity* (Oxford : Oxford University Press)
[61] Yeoh O H 1990 Characterization of elastic properties of carbon-black-filled rubber vulcanizates *Rubber Chem. Technol.* **63** 792–805
[62] Arruda E M and Boyce M C 1993 A three-dimensional constitutive model for the large stretch behavior of rubber elastic materials *J. Mech. Phys. Solids* **41** 389–412
[63] Gent A N 1996 A new constitutive relation for rubber *Rubber Chem. Technol.* **69** 59–61
[64] Kim H, Oh S, Hwang K, Choi H, Jeon J and Nam J 2001 Actuator model of electrostrictive polymers (eps) for microactuators *SPIE's 8th Annual Int. Symp. on Smart Structures and Materials* pp 482–90
[65] Goulbourne N C, Frecker M I and Mockensturm E 2004 Electro-elastic modeling of a dielectric elastomer diaphragm for a prosthetic blood pump *Smart Structures and Materials* pp 122–33
[66] Wissler M and Mazza E 2005 Modeling of a pre-strained circular actuator made of dielectric elastomers *Sensors Actuators* A **120** 184–92
[67] Plante J and Dubowsky S 2006 Large-scale failure modes of dielectric elastomer actuators *Int. J. Solids Struct.* **43** 7727–51
[68] Suo Z, Zhao X and Greene W H 2008 A nonlinear field theory of deformable dielectrics *J. Mech. Phys. Solids* **56** 467–86
[69] Zhao X and Suo Z 2007 Method to analyze electromechanical stability of dielectric elastomers *Appl. Phys. Lett.* **91** 061921
[70] Koh S, Li T, Zhou J, Zhao X, Hong W, Zhu J and Suo Z 2011 Mechanisms of large actuation strain in dielectric elastomers *J. Polym. Sci.* B **49** 504–15
[71] Wang Y, Chen B, Bai Y, Wang H and Zhou J 2014 Actuating dielectric elastomers in pure shear deformation by elastomeric conductors *Appl. Phys. Lett.* **104** 064101
[72] Joglekar M M 2014 An energy-based approach to extract the dynamic instability parameters of dielectric elastomer actuators *J. Appl. Mech.* **81** 091010
[73] Kollosche M, Zhu J, Suo Z and Kofod G 2012 Complex interplay of nonlinear processes in dielectric elastomers *Phys. Rev.* E **85** 051801
[74] Zhao X and Wang Q 2014 Harnessing large deformation and instabilities of soft dielectrics: theory, experiment, and application *Appl. Phys. Rev.* **1** 021304
[75] Li B, Zhou J and Chen H 2011 Electromechanical stability in charge-controlled dielectric elastomer actuation *Appl. Phys. Lett.* **99** 244101
[76] Wang H, Cai S, Carpi F and Suo Z 2012 Computational model of hydrostatically coupled dielectric elastomer actuators *J. Appl. Mech.* **79** 031008
[77] Gupta U, Godaba H, Zhao Z, Chui C K and Zhu J 2015 Tunable force/displacement of a vibration shaker driven by a dielectric elastomer actuator *Extreme Mech. Lett.* **287** 72–7
[78] Zhu J, Kollosche M, Lu T, Kofod G and Suo Z 2012 Two types of transitions to wrinkles in dielectric elastomers *Soft Matter* **8** 8840–6
[79] Li T, Qu S and Yang W 2012 Electromechanical and dynamic analyses of tunable dielectric elastomer resonator *Int. J. Solids Struct.* **49** 3754–61
[80] Maffli L, Rosset S and Shea H R 2013 Zipping dielectric elastomer actuators: characterization, design and modeling *Smart Mater. Struct.* **22** 104013
[81] Kollosche M, Kofod G, Suo Z and Zhu J 2015 Temporal evolution and instability in a viscoelastic dielectric elastomer *J. Mech. Phys. Solids* **76** 47–64
[82] Akbari S, Rosset S and Shea H R 2013 Improved electromechanical behavior in castable dielectric elastomer actuators *Appl. Phys. Lett.* **102** 071906
[83] Zhang J, Wang Y, McCoul D, Pei Q and Chen H 2014 Viscoelastic creep elimination in dielectric elastomer actuation by preprogrammed voltage *Appl. Phys. Lett.* **105** 212904
[84] Wang Y, Chen B, Bai Y, Wang H and Zhou J 2014 Actuating dielectric elastomers in pure shear deformation by elastomeric conductors *Appl. Phys. Lett.* **104** 064101
[85] Goulbourne N, Mockensturm E and Frecker M 2005 A nonlinear model for dielectric elastomer membranes *J. Appl. Mech.* **72** 899–906
[86] Bauer S and Paajanen M 2006 Electromechanical characterization and measurement protocol for dielectric elastomer actuators *Smart Structures and Materials*61682K
[87] Plante J S and Dubowsky S 2007 On the properties of dielectric elastomer actuators and their design implications *Smart Mater. Struct.* **16** S227

[88] Patrick L, Gabor K and Silvain M 2007 Characterization of dielectric elastomer actuators based on a hyperelastic film model *Sensors Actuators* A **135** 748–57
[89] Kofod G 2008 The static actuation of dielectric elastomer actuators: how does pre-stretch improve actuation? *J. Phys. D: Appl. Phys.* **41** 215405
[90] Ahmadi S, Gooyers M, Soleimani M and Menon C 2013 Fabrication and electromechanical examination of a spherical dielectric elastomer actuator *Smart Mater. Struct.* **22** 115004
[91] Molberg M *et al* 2009 Frequency dependent dielectric and mechanical behavior of elastomers for actuator applications *J. Appl. Phys.* **106** 054112
[92] McKay T, OBrien B, Calius E and Anderson I 2010 Self-priming dielectric elastomer generators *Smart Mater. Struct.* **19** 055025
[93] York A, Dunn J and Seelecke S 2010 Experimental characterization of the hysteretic and rate-dependent electromechanical behavior of dielectric electro-active polymer actuators *Smart Mater. Struct.* **19** 094014
[94] Park H S and Nguyen T D 2013 Viscoelastic effects on electromechanical instabilities in dielectric elastomers *Soft Matter* **9** 1031–42
[95] Zhou J, Jiang L and Khayat R E 2015 Investigation on the performance of a viscoelastic dielectric elastomer membrane generator *Soft matter* **11** 2983–92
[96] Zhu J, Cai S and Suo Z 2010 Resonant behavior of a membrane of a dielectric elastomer *Int. J. Solids Struct.* **47** 3254–62
[97] Feng C, Jiang L and Lau W M 2011 Dynamic characteristics of a dielectric elastomer-based microbeam resonator with small vibration amplitude *J. Micromech. Microeng.* **21** 095002
[98] Xu B X, Mueller R, Theis A, Klassen M and Gross D 2012 Dynamic analysis of dielectric elastomer actuators *Appl. Phys. Lett.* **100** 112903
[99] Sheng J, Chen H, Liu L, Zhang J, Wang Y and Jia S 2013 Dynamic electromechanical performance of viscoelastic dielectric elastomers *J. Appl. Phys.* **114** 134101
[100] Zhang C, Chen H, Li B, Wang Y, Liu L and Li D 2015 Investigation on static and dynamic performance of a hinge configuration with integrated dielectric elastomers *J. Appl. Polym. Sci.* **132** 41630
[101] Kaal W and Herold S 2011 Electroactive polymer actuators in dynamic applications *IEEE/ASME Trans. Mechatronics* **16** 24–32
[102] Rosset S, Gebbers P, O'Brien B M and Shea H R 2012 The need for speed *SPIE Smart Structures and Materials*834004
[103] Sarban R, Lassen B and Willatzen M 2012 Dynamic electromechanical modeling of dielectric elastomer actuators with metallic electrodes *IEEE/ASME Trans. Mechatronics* **17** 960–7
[104] Kofod G, Wirges W, Paajanen M and Bauer S 2007 Energy minimization for self-organized structure formation and actuation *Appl. Phys. Lett.* **90** 081916
[105] Conn A T and Rossiter J 2012 Towards holonomic electro-elastomer actuators with six degrees of freedom *Smart Mater. Struct.* **21** 035012
[106] Chuc N H, Thuy D V, Park J, Kim D, Koo J, Lee Y, Nam J and Choi H R 2008 A dielectric elastomer actuator with self-sensing capability *The 15th Int. Symp. on: Smart Structures and Materials and Nondestructive Evaluation and Health Monitoring*69270V
[107] Gisby T A, O'Brien B M and Anderson I A 2013 Self sensing feedback for dielectric elastomer actuators *Appl. Phys. Lett.* **102** 193703
[108] Rosset S, Brien B M O, Gisby T, Xu D, Shea H R and Anderson I A 2013 Self-sensing dielectric elastomer actuators in closed-loop operation *Smart Mater. Struct.* **22** 104018
[109] Jung K, Kim K J and Choi H R 2008 A self-sensing dielectric elastomer actuator *Sensors Actuators* A **143** 343–51
[110] Matysek M, Haus H, Moessinger H, Brokken D, Lotz P and Schlaak H F 2011 Combined driving and sensing circuitry for dielectric elastomer actuators in mobile applications *SPIE Smart Structures and Materials+ Nondestructive Evaluation and Health Monitoring*797612
[111] Rizzello G, Naso D, York A and Seelecke S 2016 Closed loop control of dielectric elastomer actuators based on self-sensing displacement feedback *Smart Mater. Struct.* **25** 035034
[112] Hoffstadt T, Griese M and Maas J 2014 Online identification algorithms for integrated dielectric electroactive polymer sensors and self-sensing concepts *Smart Mater. Struct.* **23** 104007
[113] Bar-Cohen Y 2006 Biomimetics using nature to inspire human innovation *Bioinspiration Biomimetics* **1** 1
[114] Li Z, Su C, Li G and Su H 2015 Fuzzy approximation-based adaptive backstepping control of an exoskeleton for human upper limbs *IEEE Trans. Fuzzy Syst.* **23** 555 - 566
[115] Pei Q, Rosenthal M, Stanford S, Prahlad H and Pelrine R 2004 Multiple-degrees-of-freedom electroelastomer roll actuators *Smart Mater. Struct.* **13** N86
[116] Jung M Y *et al* 2006 Fabrication and characterization of linearfabrication and characterization of linear motion dielectric elastomer actuators *Proc. SPIE* **6168** 616824–7
[117] Kovacs G, Lochmatter P and Wissler M 2007 An arm wrestling robot driven by dielectric elastomer actuators *Smart Mater. Struct.* **16** S306
[118] Biddiss E and Chau T 2008 Dielectric elastomers as actuators for upper limb prosthetics: challenges and opportunities *Med. Eng. Phys.* **30** 403–18
[119] Ashley S 2003 Artificial muscles *Sci. Am.* **289** 52–9
[120] Bar-Cohen Y 2008 Human-like robots as platforms for electroactive polymers (eap) *The 15th Int. Symp. on: Smart Structures and Materials & Nondestructive Evaluation and Health Monitoring* 692703
[121] Reitelshofer S, Landgraf M, Yoo I S, Horber J, Ramer C, Ziegler C and Franke J 2014 Dielectric elastomer actuators on the way to new actuation-systems driving future assistive, compliant and safe robots and prostheses *Proc. IEEE RAS & EMBS Int. Conf. on Biomedical Robotics and Biomechatronics* pp 803–8
[122] Carpi F, Frediani G and De Rossi D 2011 Opportunities of hydrostatically coupled dielectric elastomer actuators for haptic interfaces *Proc. SPIE* **7976** 797618
[123] Lee H S *et al* 2014 Design analysis and fabrication of arrayed tactile display based on dielectric elastomer actuator *Sensors Actuators* A **205** 191–8
[124] Knoop L E and Rossiter J 2014 Towards shear tactile displays with deas *SPIE Smart Structures and Materials+ Nondestructive Evaluation and Health Monitoring*905610
[125] Carpi D and De Rossi F 2005 Eyeball pseudo-muscular actuators for an android face *Smart Structures and Materials* pp 16–21
[126] Liu Y, Shi L, Liu L, Zhang Z and Leng J 2008 Inflated dielectric elastomer actuator for eyeball's movements: fabrication, analysis and experiments *Proc. SPIE* **6927** 69271A
[127] Carpi F, Frediani G, Turco S and De Rossi D 2011 Bioinspired tunable lens with muscle-like electroactive elastomers *Adv. Funct. Mater.* **21** 4152–8
[128] Carpi F, Fantoni G, Guerrini P and De Rossi D 2006 Buckling dielectric elastomer actuators and their use as motors for the eyeballs of an android face *Smart Structures and Materials*61681A
[129] Pelrine R *et al* 2002 Dielectric elastomer artificial muscle actuators: toward biomimetic motion *SPIE's 9th Annual Int. Symp. on Smart Structures and Materials* pp 126–37
[130] Pei Q, Pelrine R, Stanford S, Kornbluh R D, Rosenthal M S, Meijer K and Full R J 2002 Multifunctional electroelastomer rolls and their application for biomimetic walking robots *SPIE's 9th Annual Int. Symp. on Smart Structures and Materials* pp 246–53
[131] Nguyen C T *et al* 2014 A small biomimetic quadruped robot driven by multistacked dielectric elastomer actuators *Smart Mater. Struct.* **23** 065005
[132] Eckerle J, Stanford S, Marlow J, Schmidt R, Oh S, Low T and Shastri S V 2001 Biologically inspired hexapedal robot using field-effect electroactive elastomer artificial muscles *SPIE's*

8th Annual Int. Symp. on Smart Structures and Materials pp 269–80
[133] Nguyen C T, Phung H, Jung H, Kim U, Nguyen T D, Park J, Moon H, Koo J C and Choi H R 2015 Printable monolithic hexapod robot driven by soft actuator *Proc. IEEE Int. Conf. on Robotics and Automation* pp 4484–9
[134] Jung K, Koo J C, Lee Y K and Choi H R 2007 Artificial annelid robot driven by soft actuators *Bioinspiration Biomimetics* **2** S42
[135] Shian S, Bertoldi K and Clarke D R 2015 Use of aligned fibers to enhance the performance of dielectric elastomer inchworm robots *SPIE Smart Structures and Materials+ Nondestructive Evaluation and Health Monitoring*94301P
[136] Petralia M T and Wood R J 2010 Fabrication and analysis of dielectric-elastomer minimum-energy structures for highly-deformable soft robotic systems *Proc. IEEE/RSJ Int. Conf. on Intelligent Robots and Systems* pp 2357–63
[137] Lau G K, Lim H T, Teo J Y and Chin Y W 2014 Lightweight mechanical amplifiers for rolled dielectric elastomer actuators and their integration with bio-inspired wing flappers *Smart Mater. Struct.* **23** 025021
[138] Pei Q, Pelrine R, Rosenthal M A, Stanford S, Prahlad H and Kornbluh R D 2004 Recent progress on electroelastomer artificial muscles and their application for biomimetic robots *Smart Structures and Materials* pp 41–50
[139] Plante J 2006 Dielectric elastomer actuators for binary robotics and mechatronics *PhD Thesis* Massachusetts Institute of Technology
[140] Shintake J, Rosset S, Schubert B E, Floreano D and Shea H R 2015 A foldable antagonistic actuator *IEEE/ASME Trans. Mechatronics* **20** 1997–2008
[141] Laschi C, Mazzolai B, Mattoli V, Cianchetti M and Dario P 2009 Design and development of a soft actuator for a robot inspired by the octopus arm *Experimental Robotics* (Berlin: Springer) pp 25–33
[142] Godaba H, Li J, Wang Y and Zhu J 2016 A soft jellyfish robot driven by a dielectric elastomer actuator *IEEE Robot. Autom. Lett.* **1** 624–31
[143] Bar-Cohen Y 2002 Electroactive polymers as artificial muscles: a review *J. Spacecr. Rockets* **39** 822–7
[144] Chu W S, Lee K T and Song S H 2012 Review of biomimetic underwater robots using smart actuators *Int. J. Precis. Eng. Manuf.* **13** 1281–92
[145] Jo C, Pugal D, Oh I K, Kim K J and Asaka K 2013 Recent advances in ionic polymer-metal composite actuators and their modeling and applications *Prog. Polym. Sci.* **38** 1037–66
[146] Jani J M, Leary M, Subic A and Gibson M A 2014 A review of shape memory alloy research, applications and opportunities *Mater. Des.* **56** 1078–113
[147] Baitch T 1972 *Electrical Technology* (New York: Wiley)
[148] 4d sound technology enhances audio experience through physical feedback. http://madcatz.com/mad-catz-selects-vivitouch-4d-sound-technology-for-use-in-gaming-headset/.
[149] Carpi F, Frediani G, Gerboni C, Gemignani J and De Rossi D 2014 Enabling variable-stiffness hand rehabilitation orthoses with dielectric elastomer transducers *Med. Eng. Phys.* **36** 205–11
[150] Lotz P, Matysek M and Schlaak H F 2011 Fabrication and application of miniaturized dielectric elastomer stack actuators *IEEE/ASME Trans. Mechatronics* **16** 58–66
[151] Araromi O A, Rosset S and Shea H R 2015 High-resolution, large-area fabrication of compliant electrodes via laser ablation for robust, stretchable dielectric elastomer actuators and sensors *ACS Appl. Mater. Interfaces* **7** 18046–53
[152] Duduta M, Wood R J and Clarke D R 2016 Multilayer dielectric elastomers for fast, programmable actuation without prestretch *Adv. Mater.* **28** 8058-8063
[153] Yoo I S, Landgraf M, Ramer C, Reitelsh?fer S, Ziegler C and Franke J 2014 My new colleague has artificial muscles: a dea based approach for inherently compliant robotic systems *Prod. Eng.* **8** 711–7
[154] McKay T G, Rosset S, Anderson I A and Shea H 2014 Dielectric elastomer generators that stack up *Smart Mater. Struct.* **24** 015014
[155] Brien B M O, Rosset S, Anderson I A and Shea H R 2013 Ion implanted dielectric elastomer circuits *Appl. Phys.* A **111** 943–50
[156] Gu G Y, Gupta U, Zhu J, Zhu L M and Zhu X Y 2015 Feedforward deformation control of a dielectric elastomer actuator based on a nonlinear dynamic model *Appl. Phys. Lett.* **107** 042907
[157] Xie S Q, Ramson P F, Graaf D D, Calius E P and Anderson I A 2005 An adaptive control system for dielectric elastomers *Proc. IEEE Int. Conf. on Industrial Technology* pp 335–40
[158] Sarban R and Jones R W 2012 Physical model-based active vibration control using a dielectric elastomer actuator *J. Intell. Mater. Syst. Struct.* **23** 473–83
[159] Wilson E D, Assaf T, Pearson M J, Rossiter J M, Anderson S R and Porrill J 2013 Bioinspired adaptive control for artificial muscles *Biomimetic and Biohybrid Systems* (Berlin: Springer) pp 311–22
[160] Zou J, Gu G Y and Zhu L M 2016 Open-loop control of creep and vibration in dielectric elastomer actuators with phenomenological models *IEEE/ASME Trans. Mechatronics* 1–9
[161] Nguyen C H, Alici G and Mutlu R 2014 A compliant translational mechanism based on dielectric elastomer actuators *J. Mech. Des.* **136** 061009
[162] Pfeifer R, Lungarella M and Iida F 2007 Self-organization, embodiment, and biologically inspired robotics *Science* **318** 1088–93
[163] Reyhanoglu M, Van der Schaft A, McClamroch N H and Kolmanovsky I 1999 Dynamics and control of a class of underactuated mechanical systems *IEEE Trans. Autom. Control* **44** 1663–71
[164] Huang J, Guan Z H, Matsuno T, Fukuda T and Sekiyama K 2010 Sliding-mode velocity control of mobile-wheeled inverted-pendulum systems *IEEE Trans. Robot.* **26** 750–8